The Folding Propensity of α/Sulfono-γ-AA Peptidic Foldamers with Both Left- and Right-Handedness

Peng Teng
University of South Florida
Mengmeng Zheng
University of South Florida
Darrell Cerrato
University of South Florida
Yan Shi
University of South Florida
Mi Zhou
University of South Florida
Songyi Xue
University of South Florida
Wei Jiang
University of South Florida
Lukasz Wojtas
University of South Florida
Li-June Ming
University of South Florida
Yong Hu
Jianfeng Cai (jianfengcai@usf.edu)
University of South Florida

Article

Keywords: peptidic foldamers, helical handedness, molecular scaffold

Posted Date: September 2nd, 2020

DOI: https://doi.org/10.21203/rs.3.rs-64570/v1

Version of Record: A version of this preprint was published at Communications Chemistry on May 10th, 2021. See the published version at https://doi.org/10.1038/s42004-021-00496-0.

The Folding Propensity of α/Sulfono-γ-AA Peptidic Foldamers with Both Left- and Right-Handedness

Peng Teng,[†,#] Mengmeng Zheng,[†,#] Darrell Cole Cerrato,[†] Yan Shi,[†] Mi Zhou,[†] Songyi Xue,[†] Wei Jiang,[†,§] Lukasz Wojtas,[†] Li-June Ming,[†] Yong Hu,*[,§] and Jianfeng Cai*[,†]

[†]Department of Chemistry, University of South Florida, 4202 E. Fowler Ave, Tampa, FL 33620, USA

[§]College of Engineering and Applied Science, Nanjing University, Nanjing, Jiangsu, 210093, P. R. China

Abstract

The discovery and application of new types of helical peptidic foldamers have been an attractive endeavor to enable the development of new materials, catalysts and biological molecules. To maximize their application potential through structure-based design, it is imperative to control their helical handedness based on their molecular scaffold. Herein we first demonstrate the generalizability of the solid-state right-handed helical propensity of the 4_{13}-helix of L-α/L-sulfono-γ-AA peptides that as short as 11-mer, using the high-resolution X-ray single crystallography. The atomic level folding conformation of the foldamers was also elucidated by 2D NMR and circular dichroism under various conditions. Subsequently, we show that the helical handedness of this class of foldamer is controlled by the chirality of their chiral side chains, as demonstrated by the left-handed 4_{13}-helix comprising 1:1 D-α/D-sulfono-γ-AA peptide. In addition, a heterochiral coiled-coil-like structure was also revealed for the first time, unambiguously supporting the impact of chirality on their helical handedness. Our findings enable the structure-based design of

unique folding biopolymers and materials with the exclusive handedness or the racemic form of the foldamers in the future.

Introduction

For decades, the development of synthetic foldamers[1,2] that mimic the structure and function of natural biopolymers has boosted markedly. These synthetic oligomers are endowed with enhanced resistance toward proteolytic degradation and sequence diversity, along with promise in biomedical and material applications.[2] Meanwhile, akin to natural peptides, they can bind to various biomolecular targets such as proteins,[3-5] membranes,[6-9] RNAs,[10] and so on, with the ability to fold into conformationally stable structures. To date, foldamer backbone including β-peptides,[11] peptoids,[12] β-peptoids,[13] oligoureas,[14] aza-peptides,[15] α-aminoisobutyric acid (Aib),[16] oligoproline,[17] cis-β-aminocyclopropane carboxylic acids (cis-β-ACCs),[18] hybrid peptides,[19] aromatic amide foldamers,[20,21] etc., have been well established especially by crystallographic analysis, leading to fruitful applications in molecular self-assembly and recognition.[22,23] However, as the nature features an endless repertoire of structure and function, the identification and creation of new types of foldamer scaffolds is still challenging but yet to be achieved.[2] Gratifyingly, heterogeneous foldamers involved backbones containing subunits from two or even three classes of molecular scaffolds, e.g., α-peptides containing β- or γ-amino acid residues,[24,25] have emerged to be an promising strategy to significantly increase the availability of molecular structures and biological functions.[19,26] Despite the limited success of the hybrid foldamers, the development of new classes of hybrid foldamers and the precise control of their helical propensity remain largely unexplored.

Since 2011, γ-AApeptides (stemming from chiral PNA backbone[27]) have emerged as a new class of peptidomimetics with advantages of immense chemical diversity and enhanced resistance toward proteolytic degradation.[28] This class of peptidomimetics has shown robust promise in biomedical and material sciences.[29] However, it was highly challenging to understand the helical folding propensity of this type of oligomers, since they are distinct from the double helix formed by PNA/PNA or PNA/DNA which are stabilized by Watson-Crick base pairing rather than intramolecular hydrogen bonding.[30] Recently, we have reported two types of right-handed helices formed by heterogeneous 2:1 L-α/D-sulfono-γ-AA hybrid oligomers ($4.5_{16\text{-}14}$-helix)[31] and heterogeneous 1:1 L-α/L-sulfono-γ-AA hybrid oligomers (4_{13}-helix),[32] and one left-handed helix comprising homogeneous L-sulfono-γ-AA oligomers (4_{14}-helix),[33] all of which advanced our capability to gain insight of rational design in the future. Among them, 1:1 L-α/L-sulfono-γ-AA hybrid oligomers exhibit a right-handed 13-helix pattern, closely resembling that of α-helix. The exploration of this class of foldamer are expected to lead to profound application in functional materials. However, the structures of 1:1 L-α/L-sulfono-γ-AA hybrid oligomers were limited in only a few sequences on the solid state.[32,34,35] Their solution conformation, the generalizability of their folding propensity, including sequence length, both in solid and solution state, has not been systematically explored. In addition, it is known that D-peptides, as enantiomers of L-peptides, form left-handed α-helix, and thus one could postulate that 1:1 D-α/D-sulfono-γ-AA hybrids are doomed to adopt left-handed 13-helix. However, as the molecular scaffold of α/sulfono-γ-AApeptides is different from α-peptides, which contains 50% of chiral side chains and 50% of achiral sulfonyl side chains, an unambiguous folding structure is needed to support the hypothesis. Indeed, the structural

principles between L- and D-peptide partners of such foldamers could only be ideally interpretive should the atomic-resolution structural characterization of such heterochiral assemblies be achieved.[36] However, to date very few X-ray crystal structures of the racemic form derived from a α-helical peptide corresponding to the segment of the protein have been reported.[37,38]

Herein we first report our comprehensive investigation on the folding of shorter oligomers by down-sizing the recent 4_{13}-helix (heterogeneous 1:1 L-α/L-sulfono-γ-AA hybrid foldamers).[32] The difference in the folding propensity of the exact ratio of 1:1 and 1: 1+α (Figure 1a) in the solid state were both investigated. In addition, we have also successfully revealed a left-handed helical foldamer based on the unprecedented 1:1 D-α/D-sulfono-γ-AA hybrid. For the first time, the short right-handed 1:1 L-α/L-sulfono-γ-AA hybrid foldamers and the left-handed 1:1 D-α/D-sulfono-γ-AA hybrid foldamers were systematically investigated, which unambiguously strengthens the folding architecture in this class of oligomers under various circumstances. Our results demonstrated that the helical handedness of this class of foldamer is controlled by the chirality of their chiral side chains and irrelevant to achiral sulfonyl side chains. In the last, a racemic structure of 1:1 α/sulfono-γ-AA hybrid was demonstrated by the high-resolution signal crystal X-ray diffraction to show the interaction in the heterochiral coiled-coil. Our results shed light on the structure-based design of unique folding biopolymers and functional materials with individual handedness or the racemic form of the foldamers.

Results and discussion

Sequence synthesis. Based on the reported 15-mer foldamer,[32] we synthesized a series of 1:1 L-α/L-sulfono-γ-AA hybrid oligomers with the shorter length, from 8-mer to 14-mer (oligomer **1**–**7**, Figure 1b), containing the ratio of 1:1 and 1:1+α. The L-methyl-sulfono-γ-AA with a chlorobenzene sulfonyl group was selected as before to exclude the potential impact of different side chains on the folding propensity.[33] Oligomer **8**, the 15-mer reported previously,[32] was also synthesized to investigate the helical conformation in solution.

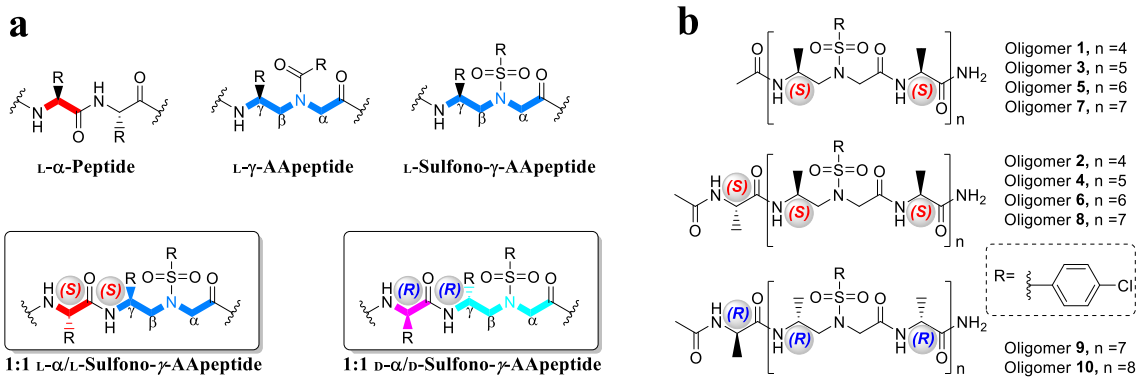

Figure 1. **Chemical structures.** (A) General structures of L-α-peptides, L-γ-AApeptides, L-sulfono-γ-AApeptides, 1:1 L-α/L-sulfono-γ-AApeptides, and 1:1 D-α/D-sulfono-γ-AApeptides. (B) 1:1 oligomer evaluated in the current study, both the exact ratio of 1:1 (**1**, **3**, **5**, and **7**) and 1: 1+α (**2**, **4**, **6**, **8**, **9** and **10**) types of oligomers were included.

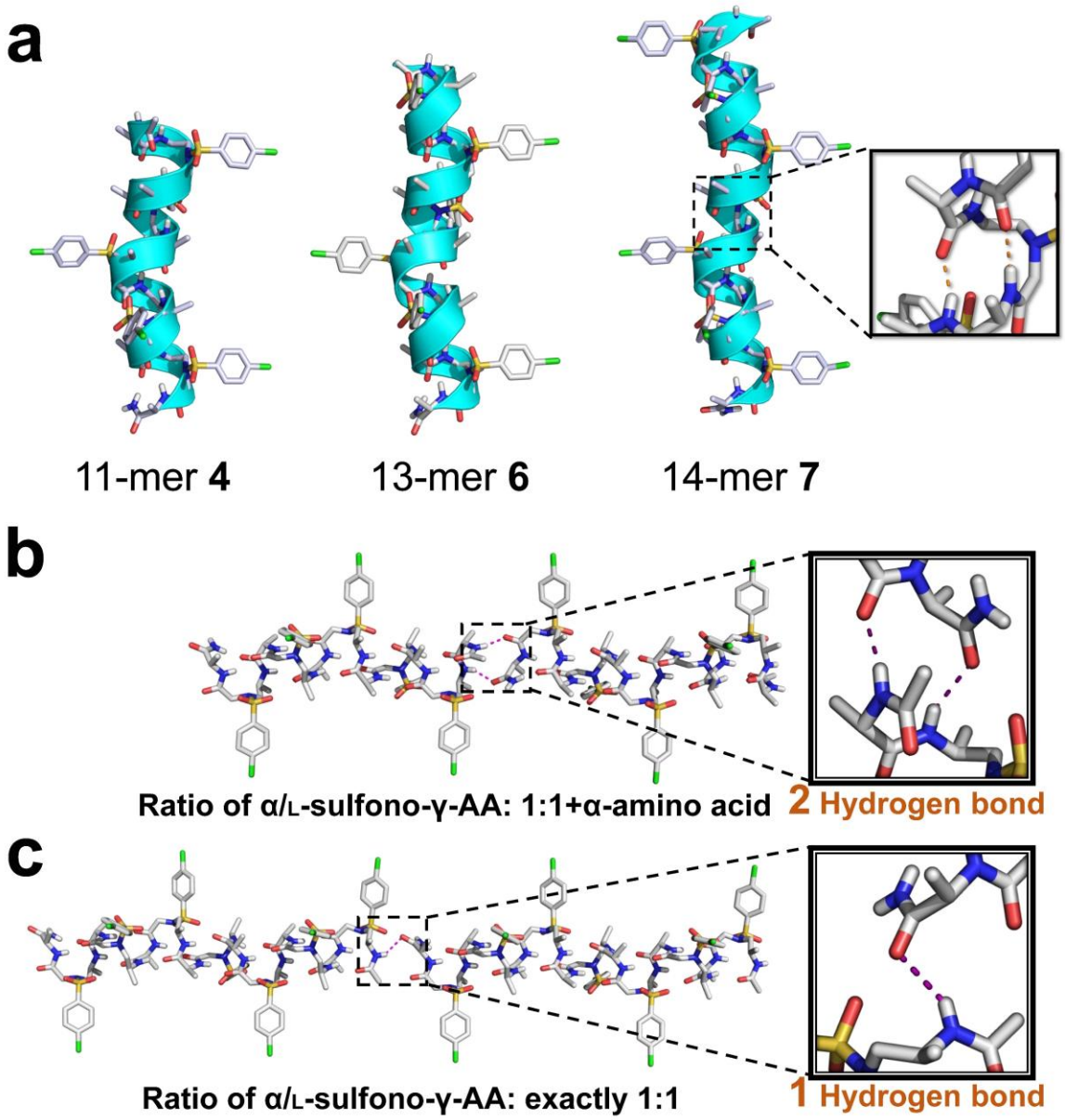

Figure 2. **Single crystal structures** (a) Single-crystal structures of 4_{13}-helix formed by 11-mer **4**, 13-mer **6**, and 14-mer **7**. The intramolecular hydrogen bond was indicated as orange dashed line in the inset. The nonpolar hydrogens were omitted for clarity. Solvent molecules were also excluded from the crystal lattice. (b) Two sets of head-to-tail intermolecular hydrogen bonding in the 1:1+α type of oligomers; (c) One set of head-to-tail intermolecular hydrogen bonding in the exactly 1:1 ratio type of oligomers. (d) A

comparison of π-helix and 4_{13}-helix. Left: a short seven residue π-helix (orange) embedded within a longer α-helix (green), taken from PDB code 3QHB. Right: a short seven residue fragment of π-helix mimetic (orange), taken from 11-mer **4**.

High-resolution crystallographic studies of oligomers 4, 6, and 7. Out of seven oligomers with incremental length (from 8-mer to 14-mer), we obtained crystals for four oligomers from different solvent systems. The 13-mer **6** crystallized readily from slow evaporation of CH_2Cl_2/CH_3CN (20:80, v/v), which are the same solvents suitable for the crystallization of 15-mer **8** but were proven unsuccessful for other oligomers. After screening various combination of solvent, we were gratified to obtain crystals for 11-mer **4** by slow diffusion of pentane into THF. To our most surprise, the 14-mer **7** bearing exact ratio of 1:1 L-α/L-sulfono-γ-AApeptides was extremely reluctant to crystal and could only crystallize from slow evaporation of chloroform, of which the access took the most challenging effort. Consequently, the crystal structures of **4**, **6**, and **7** were successfully solved by single crystal X-ray diffraction analysis with resolutions of 1.1, 1.0, and 1.3 Å, respectively. It should be noted that 11-mer (oligomer **4**) is the shortest foldamer comprising such type of backbone and with stable defined conformations in the solid state up to now. The shorter oligomer **2** (9-mer) was able to crystallize from THF/pentane multiple times but the crystals were not suitable for X-ray diffraction analysis (poor resolution about 5.00 Å), thus its structure was not solved.

Table 1. Parameters of helical structures found in proteins and foldamers consisting of sulfono-γ-AA peptide hybrids.

Secondary Structure	Backbone	Handedness	Helical Pitch p (Å)	Radius of Helix r (Å)
α-helix	L-α-peptide	Right-handed	5.4	2.3
3_{10} helix	L-α-peptide	Right-handed	6.0	1.9
π-helix	L-α-peptide	Right-handed	5.0	2.8
4.5_{16-14} helix[31]	2:1 L-α/D-sulfono-γ-AApeptide	Right-handed	5.1	2.6
4_{14} helix[33]	L-sulfono-γ-AApeptide	Left-handed	5.1	2.8
4_{13} helix	1:1 L-α/L-sulfono-γ-AApeptide	Right-handed	5.3	3.0
D-4_{13} helix	1:1 D-α/D-sulfono-γ-AApeptide	Left-handed	5.3	3.0

Despite of the various lengths of those oligomers, their crystals reveal the identically right-handed helical scaffold with even helical pitch of 5.34 Å and radius of 3.05 Å (Table 1, Figure 2a), same as that of foldamer **8**.[32] The intramolecular 13-hydrogen bindings are also as neat and uniform as the ($i \rightarrow i + 4$) hydrogen bonding pattern with distance of 1.95−2.11 Å (C=O···HN) in the 15-mer **8**. In addition, the 13-mer **6** was crystallized from the same space group $P4_12_12$ as the 15-mer **8**, however, the shorter oligomer 11-mer **4** was crystallized from $P2_1$ space group, so does the 14-mer **7**. Based on these results, we can see the oligomer that is in exact 1:1 L-α/L-sulfono-γ-AApeptide ratio is extremely challenging to crystallize. The presence of terminal α-amino acid in the 1:1+α type of oligomers prompts the crystallization of the foldamers, since it contributes to an extra set of head-to-tail intermolecular hydrogen bonding in the 1:1+α type of oligomers to aid in the packing in the crystal lattice, whereas there is only one set of head-to-tail

intermolecular hydrogen bonding exists in the exactly 1:1 type of oligomers (Figure 2b, 2c). The infinite four-pedal windmill-shaped columns along peptide axis were formed apparently, owing to the highly ordered molecular packing governed by head-to-tail intermolecular hydrogen bonds of N–H···O=C type between N- and C- terminals of helices.

In contrast to the α-helix which bears 3.6 residues/turn, these short foldamers contain exactly four side chains per turn. Their side chains are almost perpendicular to the helical axis and pointing away from the axis. Similar to those of α-helices, the side chains point toward the N-terminus in the 4_{13}-helix. Further comparison of helical pitch and radius of the 4_{13}-helix revealed that this type of helices could be potential mimetics of π-helix (Figure 2d). This is significant since π-helix only exists as very short fragments in α-helix due to its destabilization[39] on the secondary structures, while this class of foldamers is capable of forming much longer π-helix-like structures, they may lead to a new class of foldamer for π-helix mimicry.

In the direction perpendicular to the peptide axis, there exist weak interactions including C–Cl···O=C (3.2 Å, in 11-mer **4**), C–Cl···π (3.2 Å, in 11-mer **6**), C–Cl···Cl–C (3.4 Å, in 11-mer **6** and 14-mer **7**) and other Van der Waals interactions, between helices as well as between helices and solvent molecules (Figure 3). The weak interactions and helical shape of oligomers with side chlorobenzene groups drive the arrangement of adjacent helices to be parallel (**4**), antiparallel (**7**) or perpendicular (**6**), all reflected in space group symmetry. Overall, the presence of hydrogen bonds between terminal sides, shape of helices and presence of solvent molecules seem to have a primary impact on crystal

packing, particularly along with the hydrogen bonding in this class of oligomers, which may enable the design of novel functional materials even with short peptidic length.

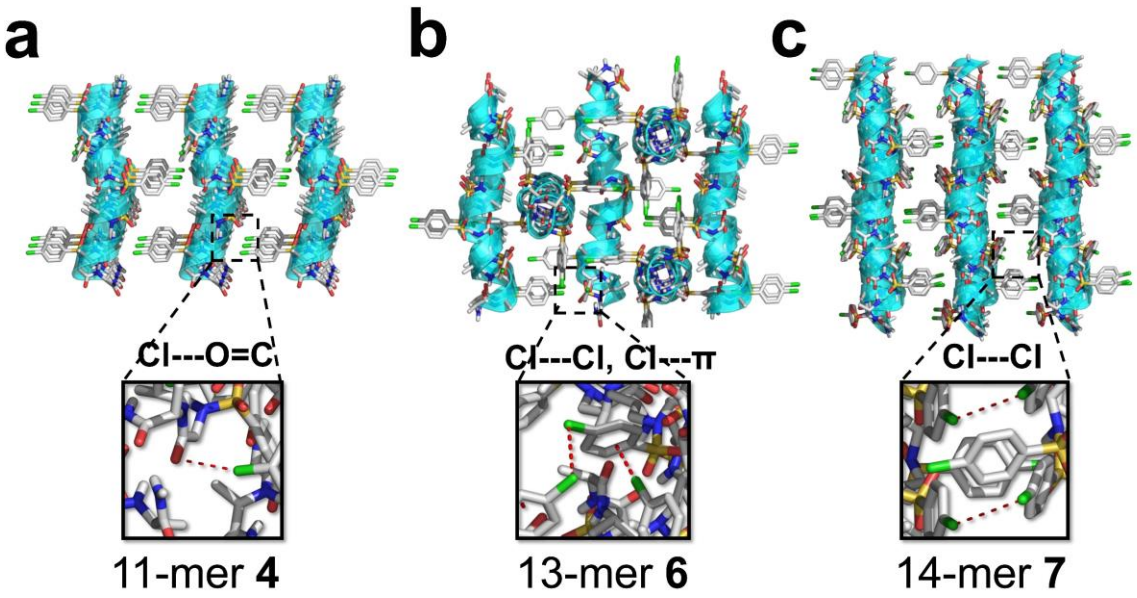

Figure 3. **Crystal packing of foldamers**. (a) Crystal packing of 11-mer **4**. (b) Crystal packing of 13-mer **6**. (c) Crystal packing of 14-mer **7**. The intermolecular Cl···O=C, C–Cl···Cl–C, and C–Cl···π interactions are indicated as red dashed line in insets.

Moreover, the mean backbone torsion angles are unambiguously revealed to be quite similar across all structures (Table 2). The torsion angles of α-Ala backbone with −73 ± 2º and −24 ± 4º for ϕ' and ψ' are different from those of neither α-Ala unit in the 4.5_{16-14} foldamers (−62 ± 3°, −39 ± 7°)[31] nor canonical α-helices (−64 ± 7°, −41 ± 7°). The torsion angles of L-sulfono-γ-AA residues with −122 ± 5º and 65 ± 7º for ϕ and θ are close to that of homogeneous L-sulfono-γ-AA backbone (−138 ± 2°, −66 ± 5°)[33], however, the backbone torsion angle η (79 ± 11°), ξ (−135 ± 6°), and ψ (4 ± 7°) are sharply distinct from those of homogeneous L-sulfono-γ-AA unit in the left-handed 4_{14}-helix (η, ξ, ψ = −120 ± 5º, 92 ±

5º, −141 ± 5°).[33] It is not surprising that the torsion angles of L-sulfono-γ-AA residues differ from those of D-sulfono-γ-AA residues in the homogeneous 4.5_{16-14} helix,[31] and reasonably different from those of β-sheet or other synthetic peptide scaffold.[40-42] This shows that the average backbone torsion angles of L-sulfono-γ-AA are globally conserved over all the structures, indicating that the folding propensity of this type of foldamers is highly unanimous and predictable. Along with the clear arrangement of the side chain, these parameters will permit the creation of either helical bundles or other defined materials, as well as the rational design of helical structure targeting membrane receptors or protein-protein interactions.

Table 2. Typical torsion angles (°) in foldamers 4, 6, 7, and 8 based on single crystals.

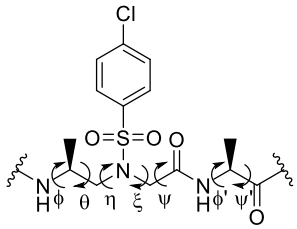

		ϕ	θ	η	ξ	ψ	ϕ'	ψ'
Right-handed	**4**	–125.4	72.3	78.9	–129.3	–3.4	–74.5	–18.5
	6	–117.2	64.4	72.1	–140.3	10.5	–72.0	–24.5
	7	–125.5	60.9	90.4	–130.2	0.6	–74.4	–28.1
	8	–118.7	61.7	75.6	–140.8	8.7	–73.1	–24.7

NMR studies of oligomer 8. To investigate the atomic-scale details of intramolecular interactions in solution, we conducted the 2D NMR of oligomer **8** at a concentration of 4 mM in CD_3OH at 10 ºC. Residue-specific assignments were achieved upon a combination of COSY, gDQFCOSY, zTOCSY and NOESY spectra.

Although the NMR spectra of the oligomer exhibited significant signal overlapping, as would be expected, due to the identical side chains through each sulfono-γ-AApeptide building blocks or α-peptide residues, we were able to assign entire protons and identify numerous nuclear Overhauser enhancements (NOEs) correlations, which unambiguously support the defined secondary structure in solution. In addition to strong *i*, *i*+1 NOE correlations between NH hydrogens (Figure 4a), the long-range *i*, *i*+2 NOE peaks exist extensively across the foldamer, including *i*, *i*+2 NOE correlations between α-peptide NH and methylene/γ-CH protons of L-sulfono-γ-AA two residues away, or between NH and CH_2/CH_3 of L-sulfono-γ-AA two residues away in either direction. The chimeric *i*, *i*+3 and *i*, *i*+4 NOE correlations were also detected among the NH protons of L-sulfono-γ-AA and CH_3 three of four residues away. These detected NOE correlations are consistent with $i \rightarrow i + 4$) hydrogen bonding pattern found in crystal structures, indicating predominant defined helical structures of the foldamer in solution.

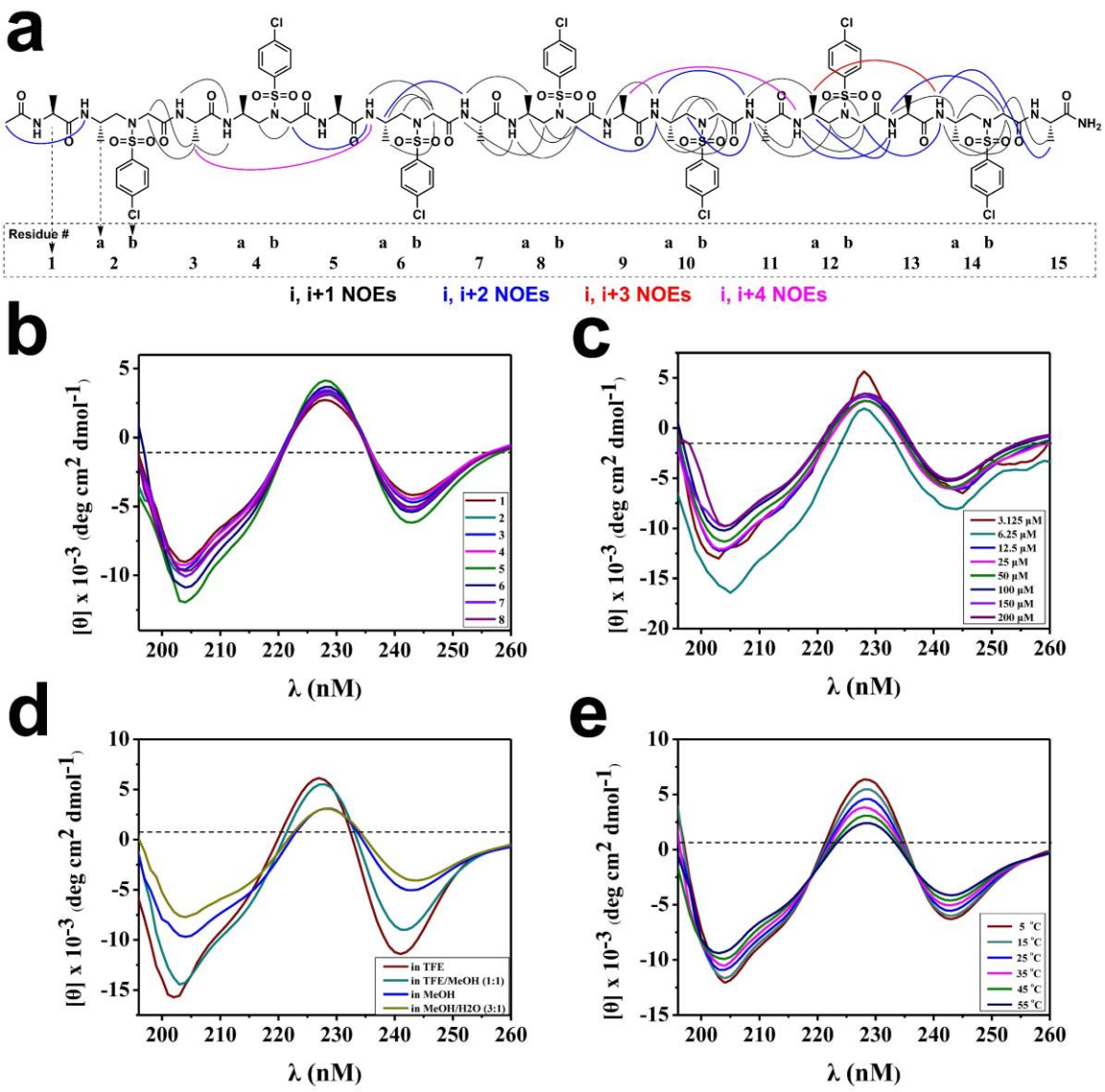

Figure 4. **Solution structures of foldamers**. (a) Summary of detected NOESY cross-peaks (200 ms mixing time) of foldamer **8** between protons on nonadjacent residues in CD_3OH (4 mM concentration, 10 °C). Four types of NOEs are displayed in different color. Each L-sulfono-γ-AA peptide unit is considered as two residues since it is equal to two α-amino acids in length. (b) CD spectra of compounds **1**–**8** (100 μM) measured at room temperature in CH_3OH. (c) CD spectra of compound **8** in CH_3OH at various concentrations

at room temperature. (d) CD spectra of compound **8** (100 μM) in various solvents at room temperature. (e) CD spectra of compound **8** (100 μM) in CH_3OH at various temperatures.

CD studies. We next conducted the circular dichroism (CD) spectroscopy of each sequence to correlate their helical structures to the CD spectra. All the eight oligomers displayed similar CD signatures in methanol, although quite different from α-helix. There is a pronounced minimum at 204 nm, similar to the behavior of a helical α/β/γ-peptide,[19] and minimum around 242 nm, meanwhile, a maximum at 228 nm (Figure 4b). The CD trend was also in good agreement with that of the heterogeneous 1:1 L-α/L-sulfono-γ-AA oligomers bearing other miscellaneous side chains.[43] These results indicate that the oligomers have similar solution structures in solution regardless of their lengths and side chains, suggesting robust folding propensity in this class of peptidomimetics.

Concentration-dependence of oligomer **8**, as well as the solvent effect on the helical stability, was also investigated. It's notable that the sequence adopts well-defined helix over the concentration ranging from 3.125 to 200 μM (Figure 4c). Moreover, it is not surprising that the sequences adopt the best helical conformations in pure trifluoroethanol (TFE) as TFE is a well-known solvent stabilizing the secondary structure, however, in the presence of water the sequence retained an intriguingly good degree of helicity, although the population is somewhat less than that in methanol (Figure 4d). Lastly, the helically thermal stability of the sequence was also evaluated by temperature-dependent CD studies. The CD spectra of **8** show no change in shape and only a slight decrease in the CD signal intensity of the minimum at 204 nm and the maximum at 228 nm over the temperature

range 5–55 °C (Figure 4e), indicating high stability of helical sequence of this type in solution.

Left-handed Foldamer. The conventional α-helices in the proteins conspicuously prefer right-handed configuration,[44] while the left-handed peptidic helices were very rare in nature,[45] although few examples on the unnatural β-peptides[46] or Aib[9,47] and a few nonpeptidic backbones based helical polymers[48] showed dynamic folding propensity. In sharp contrast, D-amino acid is uncommon in live organisms, and the contribution of D-amino acid on the helical conformation was much less investigated but remains great interest, because the helices consisting of D-amino acid resist degradation by natural proteases.[38] We have systematically demonstrated that the 1:1 α-L/L-sulfono-γ-AA hybrid adopts the right-handed helix vide supra, but it would be attractive to have the atomic level structural information of the counterpart of the right-handed helix, namely the left-handed foldamer based on the 1:1 D-α/D-sulfono-γ-AA hybrid (Figure 1b).

To this end, two oligomers D-15-mer **9** and D-17-mer **10** bearing seven or eight D-sulfono-γ-AA (while bearing eight or nine D-α-amino acid) units were synthesized and characterized by CD to examine their secondary structures. As shown in Figure 5a, oligomers **9** and **10** displayed mirror-imaged CD spectra of right-handed oligomer **8** in methanol solution, suggesting that the 1:1 D-α/D-sulfono-γ-AA hybrid did form left-handed foldamers in solution, which demonstrated the critical importance of chiral configuration in terms of affording the absolute handedness of this class of foldamers. In the following experiment, both oligomers **9** and **10** readily crystallized from CH_2Cl_2/CH_3CN with decent resolution (1.1 and 1.0 Å respectively), which allowed us to determine the atomically

structural information through the X-ray crystallography. As shown in Figure 5b and 5c, oligomers **9** and **10** formed left-handed helical structures with even helical pitch of 5.34 Å and radius of 3.05 Å, same as that found in the right-handed helixes. The same neat intramolecular 13-hydrogen bindings were shown in the left-handed helical structures. The side chains point toward the N-terminus in the left-handed 4_{13}-helix, which is the same as that of the right-handed 4_{13}-helix since they are in mirror configurations. The space group $P4_32_12$ in the reasonably left-handed helixes differs from $P4_12_12$ in the right-handed helixes. In addition, the backbone torsion angles are opposite to that of the right-handed helixes (Table 3). This data unambiguously revealed that the 1:1 D-α/D-sulfono-γ-AA hybrid could form left-handed helixes which are just the mirror counterparts of the right-handed helixes comprised of 1:1 L-α/L-sulfono-γ-AA hybrid. Such control of handedness of helicity enable more precise and versatile design of these foldamers.

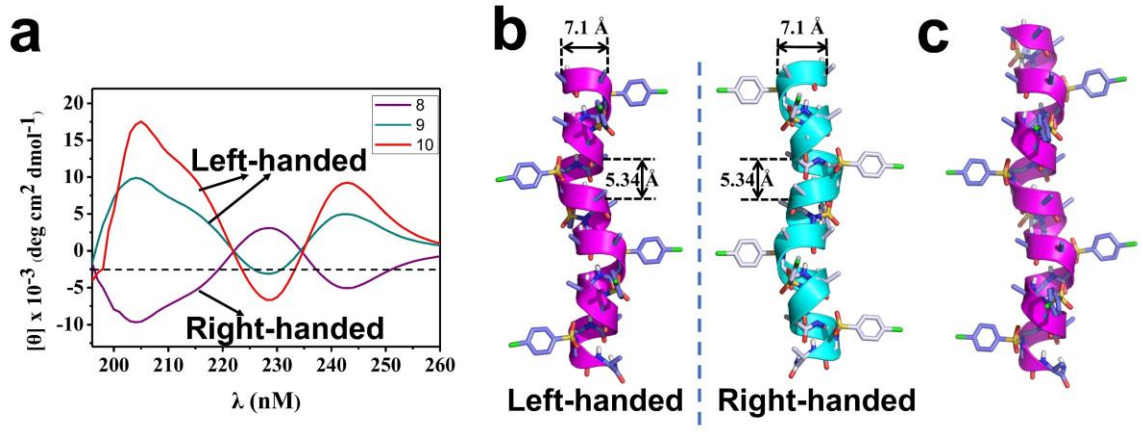

Figure 5. Left-handed foldamer (a) CD spectra of 1:1 D-α/D-sulfono-γ-AA hybrids **9** and **10** (100 μM) measured at room temperature in CH_3OH, foldamer **8** was included as a mirror comparison. (b) Single-crystal structures of left-handed helix formed by D-15-mer **9**. Single-crystal structures of right-handed helix formed by L-15-mer **8** was employed as a

mirror comparison. (c) Single-crystal structures of left-handed helix formed by D-17-mer **10**. The nonpolar hydrogens were omitted for clarity. Solvent molecules were also excluded from the crystal lattice.

Table 3. Typical torsion angles (º) in foldamers 9 and 10 based on single crystals.

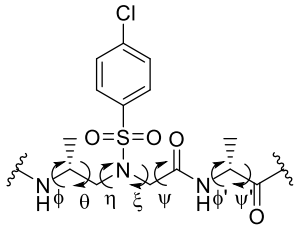

		ϕ	θ	η	ξ	ψ	ϕ'	ψ'
Right-handed	**8**	–118.7	61.7	75.6	–140.8	8.7	–73.1	–24.7
Left-handed	**9**	117.4	–62.0	–72.8	141.6	–12.5	71.4	26.1
	10	116.0	–62.2	–74.6	138.0	–5.3	69.9	25.6

The Heterochiral Coiled-Coil-Like Foldamers. Interactions between the right-handed helices with opposite absolute configurations have been a source of interest for a long time,[49,50] notably, mirror-image phage display has emerging as a powerful method to explore D-peptides as protein inhibitors.[49,51] However, the structural principles between L- and D-peptide partners remains underappreciated because of the relatively small number of atomic-resolution structural characterization. A few X-ray crystal structures of the racemic form derived from natural proteins have been reported to reveal the structural principles for the associations of L- and D-polypeptides, however, the structural information of unnatural-peptides-based heterochiral associations has not been examined.

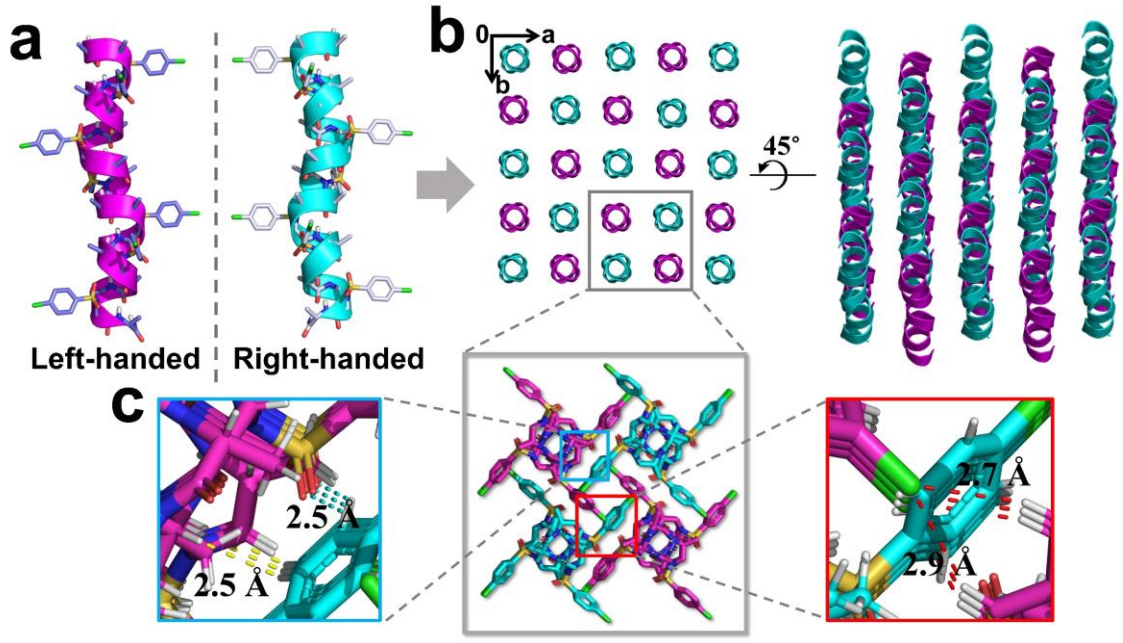

Figure 6. **Crystal structure of the heterochiral coiled-coil-like 11**. (a) Single-crystal structures of left-handed helix D-15-mer **9** and right-handed helix L-15-mer **8**. (b) The crystal structures and crystal packing of heterochiral coiled-coil formed by racemic 15-mer **11**. (c) Representative intermolecular interactions in the racemic crystals of **11**. The intermolecular C=O···H–Ph and C–H···H–Ph interactions are indicated as cyan and yellow dashed line respectively. The interhelical C–H···Cl–Ph interactions are shown as red dashed line. Solvent molecules were excluded from the crystal lattice.

Our efforts on the racemic recrystallization of foldamers **8** and **9** afforded crystals with X-ray crystal structures of 0.96 Å resolution (Figure 6a, 6b). The racemate **11** was crystallized from CH_2Cl_2/CH_3CN using slow vaporization over two days. Distinct from the oligomers with single handedness, the racemate **11** crystallized in space group $I4_1/a$. In the crystal structure, left-handed helices contact with the right-handed counterparts closer in space than the helices with single handedness (Figure 6b), akin to two gears of opposite

sense, which further manifests the impact of chiral sides chains on the helical handedness of α/sulfono-γ-AA peptides. This result is similar to the groundwork by Crick who has noticed that the helices in a heterochiral coiled-coil dimer "mesh together" in a manner akin to two gears of opposite sense.[52] In the direction of *a* and *b* axis, there are four sets of C=O···H–Ph (a distance of 2.5 Å) and C–H···H–Ph (a distance of 2.5 Å) interactions for each helix in between the surrounded helices with opposite handedness (Figure 6c). In addition, the left-handedness helices form parallel supercoils through the interhelical C–H···Cl–Ph interactions (2.7 and 2.9 Å in distance), while in the perpendicular direction, similarly parallel supercoils were formed by the right-handed helices (Figure 6b, 6c). The opposite handedness supercoils form weave-like topology in the heterochiral coiled-coil with tighter packing pattern than that in each individual component. As far as we know, the new interaction pattern has not been reported in either natural polypeptides or in the synthetic mimetics.

Conclusions

We reported the helical propensity of the 4_{13}-helix of α/sulfono-γ-AA peptide hybrid foldamers with length dependency and handedness dependency. Well-defined four-petal windmill-shaped helical conformations were strengthened in a series of foldamers with high resolution structures in both solution and solid state. The solid-state helical structure of 1:1 L-α/L-sulfono-γ-AA oligomer as short as 11-mer can be acquired by crystallographic analysis. Meanwhile, 2D NMR and CD spectroscopic data in organic solvents further support the solution structures, which are indicative of rosy folding in accordance with the atomic level high-resolution X-ray crystal structures. Moreover, the left-handed 1:1 D-α/D-

sulfono-γ-AA hybrid foldamers were revealed unambiguously at the atomic level for the first time to prove the seminal proposal. Notably, the racemate of the foldamer forms a heterochiral coiled-coil-like dimer meshing together in a manner akin to two gears of opposite sense. Our findings showed the exquisite control of handedness on this type of heterogeneous backboned peptidic foldamers by chirality manipulation of monomeric building block, which is irrelevant to achiral sulfonyl side chains. The heterochiral coiled-coil dimer also reveals *de novo* interaction model which represents a starting point for understanding and structural designing associations of tertiary or quaternary assemblies.

Materials and methods

General procedure for oligomer synthesis. The sulfono-γ-AApeptide building block synthesized as previously reported[31,32]]. All oligomers were synthesized on solid support Rink-amide resin, as in previously reported standard procedures[32]]. Full details of the chemical synthesis and purification are given in the Supplementary Information.

NMR spectroscopy. The NMR spectra were obtained on a Varian VNMRS 600 MHz spectrometer equipped with four RF channels and a Z-axis-pulse-field gradient cold probe. Sample **8** was measured at a concentration of 4.0 mM in 500 μL CD_3OH in a 5 mm NMR tube. The ^1H shift assignment was achieved by sequential assignment procedures based on DQFCOSY, COSY, zTOCSY and NOESY measurement. TOCSY and NOESY spectra were acquired with the Wet solvent suppression. All experiments were performed by collecting 4096 points in f2 and 512 points in f1. A DIPSI2 spin lock sequence with a spin lock field of 6k Hz and mixing time of 80 ms were used in zTOCSY. NOESY experiment

was carried out using a mix time of 300 ms. Further details of NMR experimental are given in the Supplementary Information.

Circular dichroism. Circular Dichroism (CD) spectra were measured on an Aviv 215 circular dichroism spectrometer using a 1 mm path length quartz cuvettes, and compound solutions in methanol were prepared using dry weight of the lyophilized solid followed by dilution to give the desired concentrations and solvent combination. 10 scans were averaged for each sample, and 3 times of independent experiments were carried out and the spectra were averaged. The final spectra were normalized by subtracting the average blank spectra.

X-ray crystallography. Lyophilized powders of oligomers **6** (3 mg), **9** (3 mg) and **10** (2 mg) were dissolved in 2 mL of dichloromethane/acetonitrile (20:80, v/v) and then left for slow evaporation at room temperature within two days to give crystals. Lyophilized powders of oligomers **4** (2 mg) were dissolved in THF (2 mL) and then pentane (1 mL) was diffused slowly into THF layer, crystals were formed in a week. Crystals of **7** were obtained from slow evaporation of 3 mg/mL solution in chloroform. Oligomers **2** was also crystalized from slow diffusion of pentane into THF in ten days, however, the crystals were not of good quality for X-ray diffraction (diffraction up to 5.00 Å of resolution only). Foldamers **8** and **9** in 1:1 ratio (4 mg, the racemate **11**) was crystallized from CH_2Cl_2/CH_3CN (60:40, v/v) using slow vaporization over two days. Details of crystallization, data collection and refinement are given in the Supplementary Information.

Data availability

The authors declare that the data supporting the findings of this study are available within the paper and its Supplementary Information files. The X-ray crystal structures of oligomer **4**, **6**, **7**, **9**, **10**, and **11** have been deposited to the CCDC database (deposition numbers CCDC 1541638, 1541639, 1541640, 1976022, 1976024, and 1976034 respectively) and are available as Supplementary Data. Any other datasets are available from the corresponding author on reasonable request.

References

1 Horne, W. S. & Gellman, S. H. Foldamers with Heterogeneous Backbones. *Acc. Chem. Res.* **41**, 1399–1408, (2008).

2 Goodman, C. M., Choi, S., Shandler, S. & DeGrado, W. F. Foldamers as versatile frameworks for the design and evolution of function. *Nat. Chem. Biol.* **3**, 252–262, (2007).

3 Gademann, K., Ernst, M., Hoyer, D. & Seebach, D. Synthesis and Biological Evaluation of a Cyclo-β-tetrapeptide as a Somatostatin Analogue. *Angew. Chem., Int. Ed.* **38**, 1223–1226, (1999).

4 Sadowsky, J. D. *et al.* Chimeric (α/β + α)-Peptide Ligands for the BH3-Recognition Cleft of Bcl-xL: Critical Role of the Molecular Scaffold in Protein Surface Recognition. *J. Am. Chem. Soc.* **127**, 11966–11968, (2005).

5 Kritzer, J. A., Lear, J. D., Hodsdon, M. E. & Schepartz, A. Helical β-Peptide Inhibitors of the p53-hDM2 Interaction. *J. Am. Chem. Soc.* **126**, 9468–9469, (2004).

6 Hamuro, Y., Schneider, J. P. & DeGrado, W. F. De Novo Design of Antibacterial β-Peptides. *J. Am. Chem. Soc.* **121**, 12200–12201, (1999).

7 Porter, E. A., Wang, X., Lee, H.-S., Weisblum, B. & Gellman, S. H. Antibiotics: Non-haemolytic [beta]-amino-acid oligomers. *Nature* **404**, 565–565 (2000).

8 Patch, J. A. & Barron, A. E. Helical Peptoid Mimics of Magainin-2 Amide. *J. Am. Chem. Soc.* **125**, 12092–12093, (2003).

9 De Poli, M. *et al.* Conformational photoswitching of a synthetic peptide foldamer bound within a phospholipid bilayer. *Science* **352**, 575–580, (2016).

10 Gelman, M. A. *et al.* Selective Binding of TAR RNA by a Tat-Derived β-Peptide. *Org. Lett.* **5**, 3563–3565, (2003).

11 Cheng, R. P., Gellman, S. H. & DeGrado, W. F. β-Peptides: From Structure to Function. *Chem. Rev.* **101**, 3219–3232, (2001).

12 Simon, R. J. *et al.* Peptoids: a modular approach to drug discovery. *Proc. Natl. Acad. Sci. U.S.A.* **89**, 9367–9371, (1992).

13 Laursen, J. S., Harris, P., Fristrup, P. & Olsen, C. A. Triangular prism-shaped beta-peptoid helices as unique biomimetic scaffolds. *Nat. Commun.* **6**, 7013, (2015).

14 Fischer, L. *et al.* The canonical helix of urea oligomers at atomic resolution: insights into folding-induced axial organization. *Angew. Chem., Int. Ed.* **49**, 1067–1070, (2010).

15 Malachowski, W. P., Tie, C., Wang, K. & Broadrup, R. L. The Synthesis of Azapeptidomimetic β-Lactam Molecules as Potential Protease Inhibitors. *J. Org. Chem.* **67**, 8962–8969, (2002).

16 Jones, J. E. *et al.* Length-Dependent Formation of Transmembrane Pores by 310-Helical alpha-Aminoisobutyric Acid Foldamers. *J. Am. Chem. Soc.* **138**, 688–695, (2016).

17 Wilhelm, P., Lewandowski, B., Trapp, N. & Wennemers, H. A crystal structure of an oligoproline PPII-helix, at last. *J. Am. Chem. Soc.* **136**, 15829–15832, (2014).

18 De Pol, S., Zorn, C., Klein, C. D., Zerbe, O. & Reiser, O. Surprisingly Stable Helical Conformations in α/β-Peptides by Incorporation of cis-β-Aminocyclopropane Carboxylic Acids. *Angew. Chem., Int. Ed.* **43**, 511–514, (2004).

19 Sawada, T. & Gellman, S. H. Structural mimicry of the alpha-helix in aqueous solution with an isoatomic alpha/beta/gamma-peptide backbone. *J. Am. Chem. Soc.* **133**, 7336–7339, (2011).

20 Garric, J., Leger, J. M. & Huc, I. Molecular apple peels. *Angew. Chem., Int. Ed.* **44**, 1954–1958, (2005).

21 Zhang, D. W., Zhao, X., Hou, J. L. & Li, Z. T. Aromatic amide foldamers: structures, properties, and functions. *Chem. Rev.* **112**, 5271–5316, (2012).

22 De Santis, E. & Ryadnov, M. G. Peptide self-assembly for nanomaterials: the old new kid on the block. *Chem. Soc. Rev.* **44**, 8288–8300, (2015).

23 Hu, Y. *et al.* Spatiotemporal control of the creation and immolation of peptide assemblies. *Coord. Chem. Rev.* **320-321**, 2–17, (2016).

24 Baldauf, C., Günther, R. & Hofmann, H.-J. Helix Formation in α,γ- and β,γ-Hybrid Peptides: Theoretical Insights into Mimicry of α- and β-Peptides. *The Journal of Organic Chemistry* **71**, 1200–1208, (2006).

25 Johnson, L. M. *et al.* Enhancement of alpha-helix mimicry by an alpha/beta-peptide foldamer via incorporation of a dense ionic side-chain array. *J. Am. Chem. Soc.* **134**, 7317–7320, (2012).

26 Pendem, N. *et al.* Controlling helix formation in the gamma-peptide superfamily: heterogeneous foldamers with urea/amide and urea/carbamate backbones. *Angew. Chem., Int. Ed.* **52**, 4147–4151, (2013).

27 Nielsen, P., Egholm, M., Berg, R. & Buchardt, O. Sequence-selective recognition of DNA by strand displacement with a thymine-substituted polyamide. *Science* **254**, 1497–1500, (1991).

28 Shi, Y. *et al.* gamma-AApeptides: Design, Structure, and Applications. *Acc. Chem. Res.* **49**, 428–441, (2016).

29 Teng, P. *et al.* Identification of novel inhibitors that disrupt STAT3-DNA interaction from a gamma-AApeptide OBOC combinatorial library. *Chem. Commun.* **50**, 8739–8742, (2014).

30 Wittung, P., Nielsen, P. E., Buchardt, O., Egholm, M. & Norden, B. DNA-like double helix formed by peptide nucleic acid. *Nature* **368**, 561–563 (1994).

31 Teng, P. *et al.* Right-Handed Helical Foldamers Consisting of De Novo d-AApeptides. *J. Am. Chem. Soc.* **139**, 7363–7369, (2017).

32 Teng, P. *et al.* Hydrogen-Bonding-Driven 3D Supramolecular Assembly of Peptidomimetic Zipper. *J. Am. Chem. Soc.* **140**, 5661–5665, (2018).

33 She, F. *et al.* De Novo Left-Handed Synthetic Peptidomimetic Foldamers. *Angew. Chem., Int. Ed.* **57**, 9916–9920, (2018).

34 Shi, Y. *et al.* Helical Sulfono-gamma-AApeptides with Aggregation-Induced Emission and Circularly Polarized Luminescence. *J. Am. Chem. Soc.* **141**, 12697–12706, (2019).

35 Teng, P. *et al.* Orthogonal Halogen-Bonding-Driven 3D Supramolecular Assembly of Right-Handed Synthetic Helical Peptides. *Angew. Chem., Int. Ed.* **58**, 7778–7782, (2019).

36 Shepherd, N. E., Hoang, H. N., Abbenante, G. & Fairlie, D. P. Left- and Right-Handed Alpha-Helical Turns in Homo- and Hetero-Chiral Helical Scaffolds. *J. Am. Chem. Soc.* **131**, 15877–15886, (2009).

37 Mortenson, D. E. *et al.* High-resolution structures of a heterochiral coiled coil. *Proc. Natl. Acad. Sci. U. S. A.* **112**, 13144–13149, (2015).

38 Kreitler, D. F. *et al.* A Hendecad Motif Is Preferred for Heterochiral Coiled-Coil Formation. *J. Am. Chem. Soc.* **141**, 1583–1592, (2019).

39 Keefe, L. J., Sondek, J., Shortle, D. & Lattman, E. E. The alpha aneurism: a structural motif revealed in an insertion mutant of staphylococcal nuclease. *Proc. Natl. Acad. Sci. U. S. A.* **90**, 3275–3279, (1993).

40 Stringer, J. R., Crapster, J. A., Guzei, I. A. & Blackwell, H. E. Extraordinarily robust polyproline type I peptoid helices generated via the incorporation of alpha-chiral aromatic N-1-naphthylethyl side chains. *J. Am. Chem. Soc.* **133**, 15559–15567, (2011).

41 Baldauf, C., Günther, R. & Hofmann, H.-J. Mixed Helices—A General Folding Pattern in Homologous Peptides? *Angew. Chem., Int. Ed.* **43**, 1594–1597, (2004).

42 Choi, S. H., Guzei, I. A., Spencer, L. C. & Gellman, S. H. Crystallographic Characterization of Helical Secondary Structures in 2:1 and 1:2 α/β-Peptides. *J. Am. Chem. Soc.* **131**, 2917–2924, (2009).

43 Wu, H. *et al.* New Class of Heterogeneous Helical Peptidomimetics. *Org. Lett.* **17**, 3524–3527, (2015).

44 Mason, S. F. Origins of biomolecular handedness. *Nature* **311**, 19–23, (1984).

45 Jagadeesh, B. *et al.* Formation of left-handed helices in hybrid peptide oligomers with cis β-sugar amino acid and l-Ala as building blocks. *Chem. Commun.*, 371–373, (2007).

46 Shin, S., Lee, M., Guzei, I. A., Kang, Y. K. & Choi, S. H. 12/10-Helical β-Peptide with Dynamic Folding Propensity: Coexistence of Right- and Left-Handed Helices in an Enantiomeric Foldamer. *J. Am. Chem. Soc.* **138**, 13390–13395, (2016).

47 Hummel, R.-P., Toniolo, C. & Jung, G. Conformational Transitions between Enantiomeric 310-Helices. *Angew. Chem., Int. Ed.* **26**, 1150–1152, (1987).

48 Yashima, E., Maeda, K. & Okamoto, Y. Memory of macromolecular helicity assisted by interaction with achiral small molecules. *Nature* **399**, 449, (1999).

49 Schumacher, T. N. M. *et al.* Identification of D-Peptide Ligands Through Mirror-Image Phage Display. *Science* **271**, 1854–1857, (1996).

50 Mandal, K. *et al.* Chemical synthesis and X-ray structure of a heterochiral {D-protein antagonist plus vascular endothelial growth factor} protein complex by racemic crystallography. *Proc. Natl. Acad. Sci. U.S.A.* **109**, 14779–14784, (2012).

51 Liu, M. *et al.* D-peptide inhibitors of the p53–MDM2 interaction for targeted molecular therapy of malignant neoplasms. *Proc. Natl. Acad. Sci. U.S.A.* **107**, 14321–14326, (2010).

52 Crick, F. H. C. The packing of α-helices: simple coiled-coils. *Acta Crystallogr.* **6**, 689–697, (1953).

Acknowledgements

This work was generously supported by NSF CAREER 1351265 (J.C.), NIH 1R01GM112652-01A1 (J.C.), and NIH 1R01AG056569-01 (J.C.).

Author Contributions

P.T., M.-M. Z. and J. C. conceived and directed the project and wrote the manuscript. P. T., M.-M. Z., S. X., and W. J. performed the synthesis, purification and characterization. P. T. and M.-M. Z. obtained the crystals. D.-C. C. run the 2D NMR experiments and resolved 2D NMR spectra. Y. S. and M. Z. carried out the CD experiments. L. W. collected crystal data and solved the crystal structures. L.-J. M. and Y. H. corrected the manuscript. #P.T. and M.Z. contributed equally to this work.

ORCID

Peng Teng: 0000-0002-7412-9646

Jianfeng Cai: 0000-0003-3106-3306

Competing interests

The authors declare no competing interests.

Additional information

Supporting Information is available for this paper at….

Experimental procedures and characterization of all sequences; Detailed 2D NMR, protons assignment and summary of NOEs; Crystal packing of four samples; Crystal data and structure refinement of four samples (PDF)

Crystallographic data of oligomer **4** (CIF)

Crystallographic data of oligomer **6** (CIF)

Crystallographic data of oligomer **7** (CIF)

Crystallographic data of oligomer **9** (CIF)

Crystallographic data of oligomer **10** (CIF)

Crystallographic data of heterochiral coiled-coil **11** (CIF)

Correspondence and requests for materials should be addressed to J. C. (jianfengcai@usf.edu) or Y. H. (hvyong@nju.edu.cn)

Supporting Information for

The Folding Propensity of α/Sulfono-γ-AA Peptidic Foldamers with Both Left- and Right-Handedness

Peng Teng,[†,#] Mengmeng Zheng,[†,#] Darrell Cole Cerrato,[†] Yan Shi,[†] Mi Zhou,[†] Songyi Xue,[†] Wei Jiang,[†,§] Lukasz Wojtas,[†] Li-June Ming,[†] Yong Hu,*[,§] and Jianfeng Cai*[,†]

[†]Department of Chemistry, University of South Florida, 4202 E. Fowler Ave, Tampa, FL 33620, USA

[§]College of Engineering and Applied Science, Nanjing University, Nanjing, Jiangsu, 210093, P. R. China

Table of Contents

1. Chemistry

All reagents and solvents were purchased from Fisher or Aldrich and used without further purification. Fmoc protected α-amino acids and Rink-amide resin (0.6 mmol/g, 200–400 mesh) were purchased from Chem-Impex International, Inc. Solid-phase syntheses of the compounds were carried out in the peptide synthesis vessel on a Burrell Wrist-Action shaker. The products were analyzed and purified on a Waters Breeze 2 HPLC system installed with both analytic module (1 mL/min) and preparative module (16 mL/min), by employing a method using 5–100% linear gradient of solvent B (0.1% TFA in acetonitrile) in solvent A (0.1% TFA in water) over 40 min, followed by 100% solvent B over 10 min. The desired fractions were collected and lyophilized on a Labconco lyophilizer. High-resolution MS was conducted on an Agilent 6540 LC/QTOF system. ^{1}HNMR spectra were acquired with the WET solvent suppression at Varian 600 MHz.

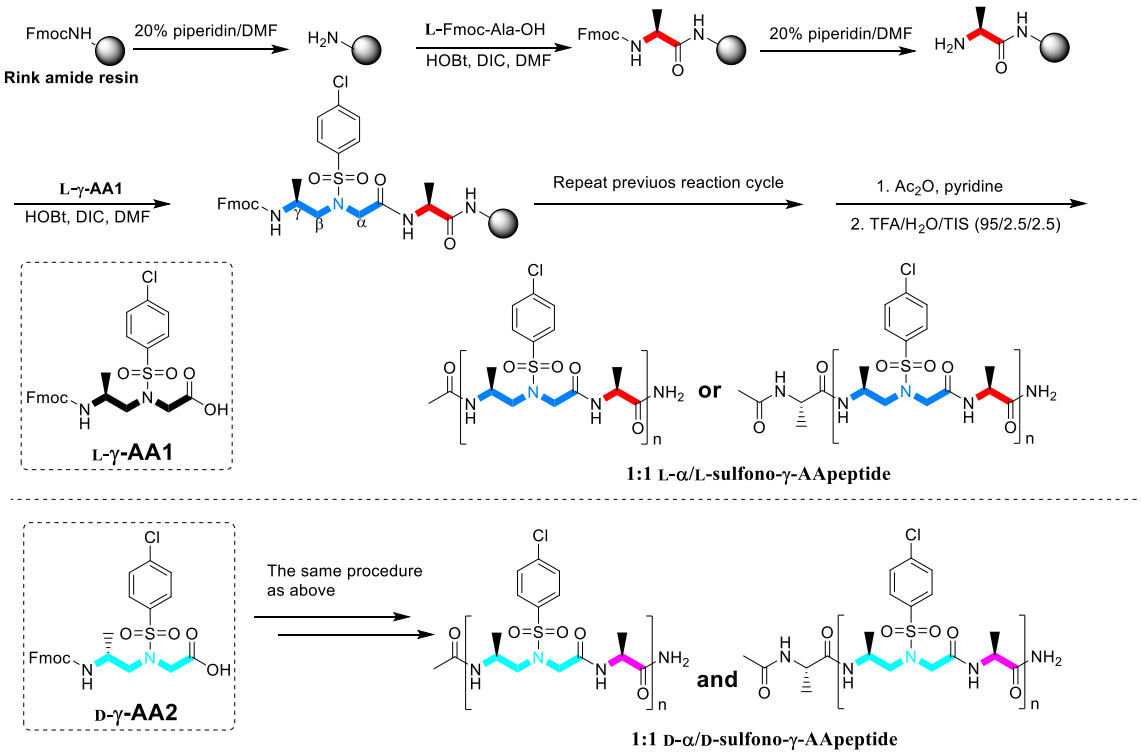

Scheme S1. General synthetic route to prepare L-α/L-sulfono-γ-AA oligomers and D-α/D-sulfono-γ-AA oligomers.

The L-sulfono-γ-AApeptide building block L-**γ-AA1** was synthesized as previously reported.(*1*) The D-sulfono-γ-AApeptide building block D-**γ-AA2** was synthesized using same procedures except that the D-Fmoc-Ala-OH was used at the beginning.(*2*) Oligomers **1**–**10** were synthesized on solid support Rink-amide resin, as shown in previously reported standard procedures.(*1-3*) 100 mg of Rink-amide resin were used for the synthesis of each oligomer.

General synthetic procedure of solid phase synthesis of oligomers. The solid phase synthesis was conducted on 100 mg Rink amide resin (0.6 mmol/g) for each oligomer under room temperature at atmosphere pressure. The resin was swelled in DMF for 30 min before use, followed by treatment with 20% piperidine/DMF solution (2 mL) for 10 min (×2) to remove Fmoc protecting group, then washed three times with DCM and three times with DMF. A premixed solution of Fmoc-Ala-OH (with desired chiral configuration**,** 3 equiv.), HOBt (6 equiv.), and DIC (6 equiv.) in 2 mL DMF was added to the resin and shaken for 4 h to complete the coupling reaction. After wash with DCM and DMF, the resin was treated with 20% piperidine/DMF solution for 10 min (×2). Then, the sulfono-γ-AApeptide building block **γ-AA** with the desired chiral configuration was coupled on the resin under the same abovementioned reaction conditions. The reaction cycles were repeated until the desired oligomers were synthesized. The N-terminal of the sequence was capped with acetic anhydride (0.5 mL) in pyridine (2 mL) (30 min×2), followed by treatment with TFA/H_2O/TIS (4 mL, 95/2.5/2.5, v/v/v) for 2 h. The cleavage solution was collected and the beads was washed with TFA (1 mL×2) and DCM (3 mL×2), the combined organic phase was evaporated under nitrogen flow to give the crude, which was analyzed and then purified by Water HPLC system, with 1 mL/min and 16 mL/min flow speed respectively. The gradient eluting method of 20% to 100% of solvent B (0.1% TFA in acetonitrile) in A (0.1% TFA in water) over 50 min was performed. All the oligomers were obtained with decent crude purity and good yield (55.88–67.04%) after prep-HPLC purification.

Oligomer **1**, HR-MS (ESI), $C_{58}H_{78}Cl_4N_{13}O_{17}S_4$ $[M+H]^+$ calcd = 1496.3270; found = 1496.3268.

Oligomer **2**, HR-MS (ESI), $C_{61}H_{83}Cl_4N_{14}O_{18}S_4$ $[M+H]^+$ calcd = 1567.3641; found = 1567.3637.

Oligomer **3**, HR-MS (ESI), $C_{72}H_{96}Cl_5N_{16}O_{21}S_5$ $[M+H]^+$ calcd = 1855.3977; found = 1855.3951.

Oligomer **4**, HR-MS (ESI), $C_{75}H_{101}Cl_5N_{17}O_{22}S_5$ $[M+H]^+$ calcd = 1926.4348; found = 1926.4308.

Oligomer **5**, HR-MS (ESI), $C_{86}H_{114}C_{l6}N_{19}O_{25}S_6$ $[M+H]^+$ calcd = 2214.4683; found = 2214.4624.

Oligomer **6**, HR-MS (ESI), $C_{89}H_{119}Cl_6N_{20}O_{26}S_6$ $[M+H]^+$ calcd = 2285.5054; found = 1145.2409 $[M+2H]^{2+}$, 1167.2321 $[M+2Na]^{2+}$.

Oligomer **7**, HR-MS (ESI), $C_{100}H_{132}Cl_7N_{22}O_{29}S_7$ $[M+Na]^+$ calcd = 2595.5209; found = 2595.5181.

Oligomer **9**, HR-MS (ESI), $C_{103}H_{136}Cl_7N_{23}O_{30}S_7$ $[M+H]^+$ calcd = 2643.5688; found = 1322.7923 $[M+2H]^{2+}$, 1345.7630 $[M+2Na]^{2+}$, 883.5293 $[M+3H]^{3+}$.

Oligomer **10**, HR-MS (ESI), $C_{117}H_{154}Cl_8N_{26}O_{34}S_8$ $[M+H]^+$ calcd = 3002.6395; found = 1504.8253 $[M+2H]^{2+}$, 1525.7979 $[M+2Na]^{2+}$, 1003.8857 $[M+3H]^{3+}$.

Table S1. HPLC purities and retention time of foldamers **1**–**10**.

Compound	HPLC purification (%)	Retention Time (min)
1	99.99	16.55
2	99.80	16.06
3	99.32	18.47
4	99.90	18.30
5	100.0	19.81
6	99.25	19.24
7	97.30	21.31
8	99.10	21.61
9	97.94	21.03
10	98.02	22.59

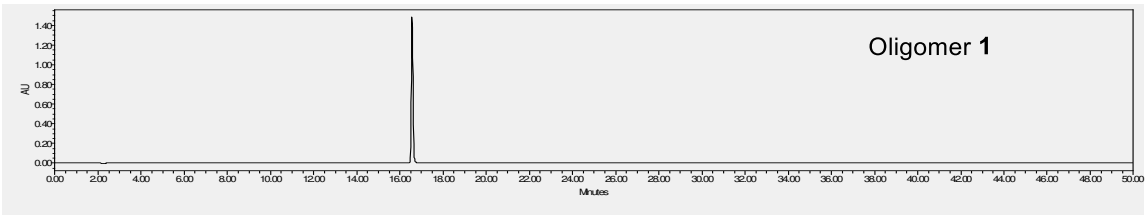
Oligomer **1**
AU
Minutes

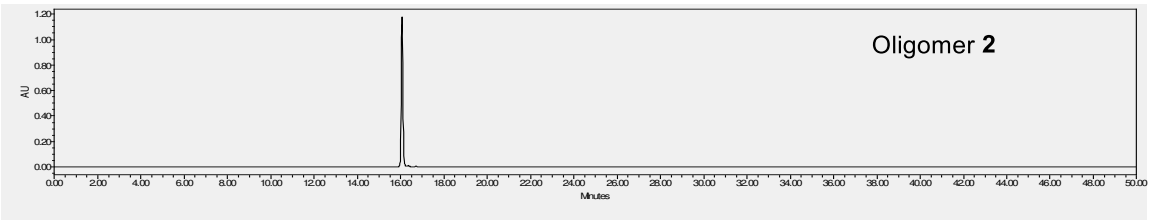
Oligomer **2**
AU
Minutes

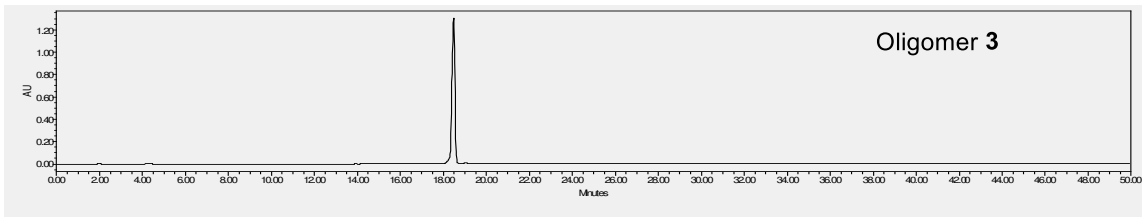
Oligomer **3**
AU
Minutes

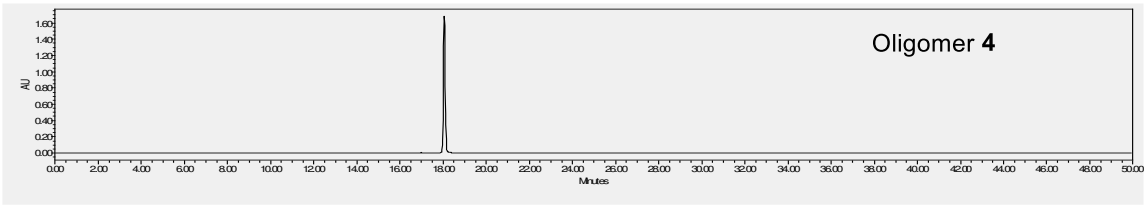
Oligomer **4**
AU
Minutes

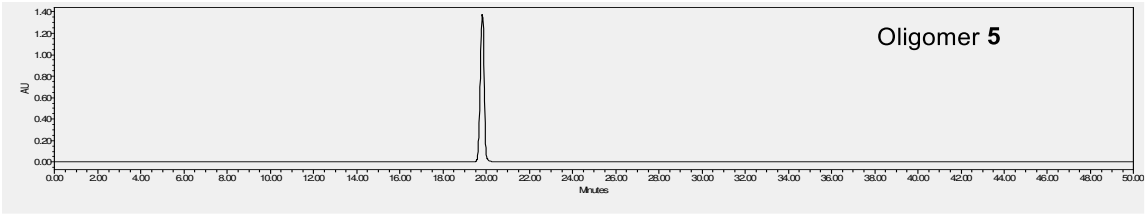
Oligomer **5**
AU
Minutes

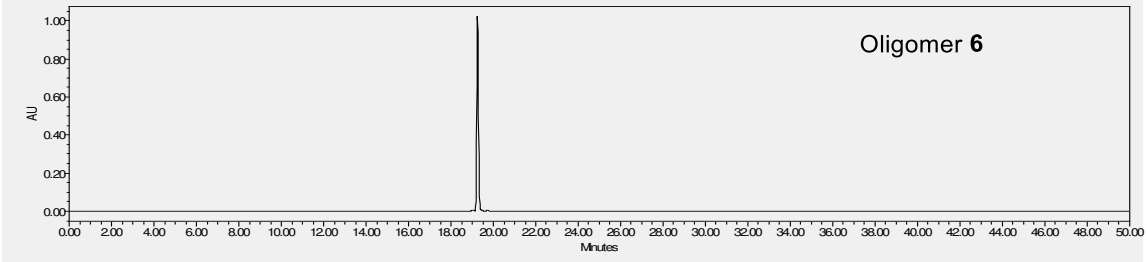
Oligomer **6**
AU
Minutes

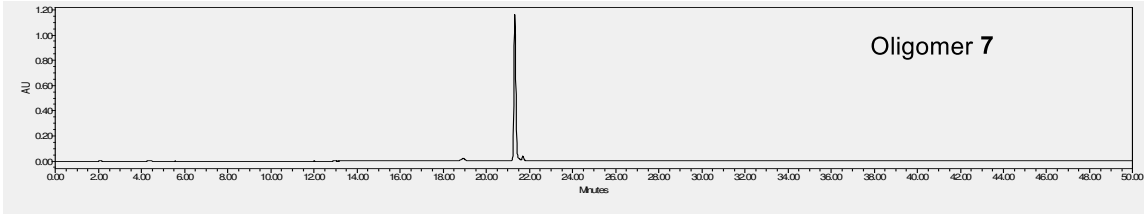
Oligomer **7**
AU
Minutes

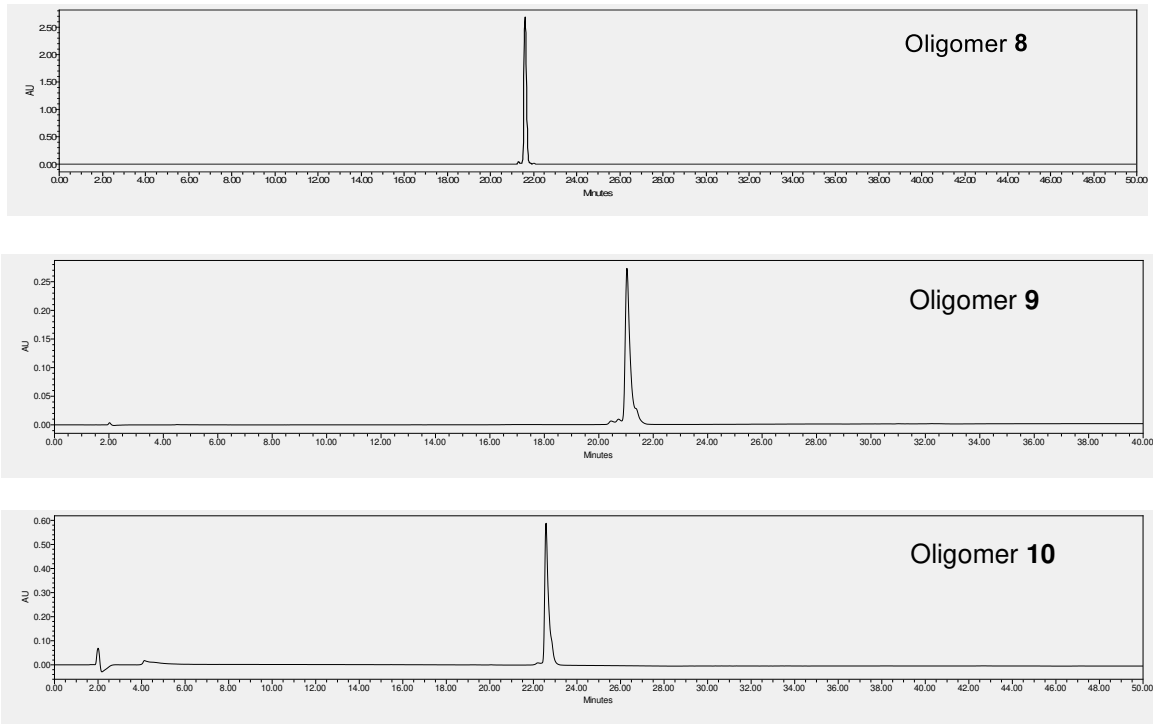

Figure S1. HPLC spectra of foldamers **1**–**10**.

Oligomer **1**

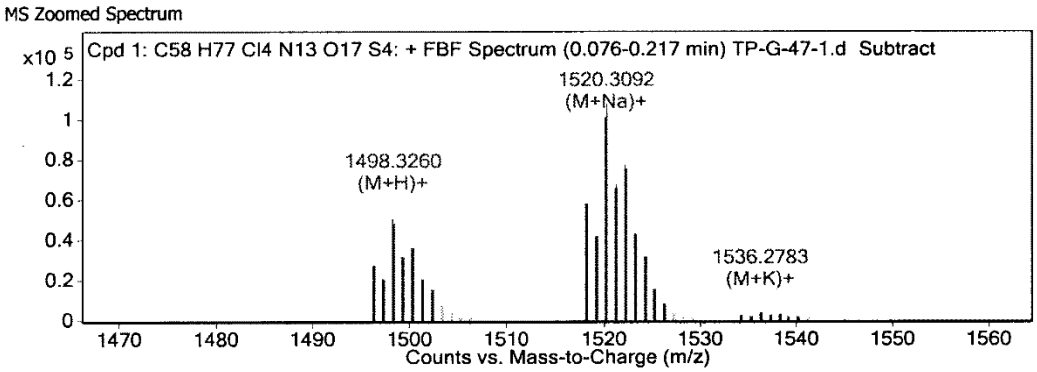

Oligomer **2**

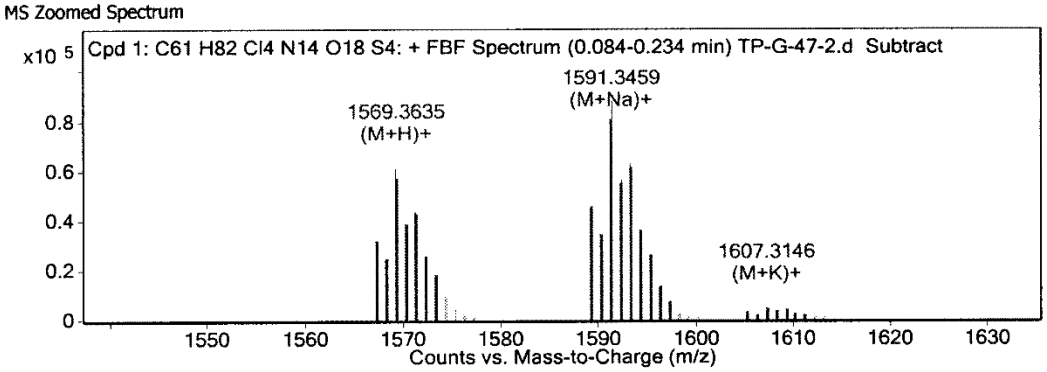

Oligomer **3**

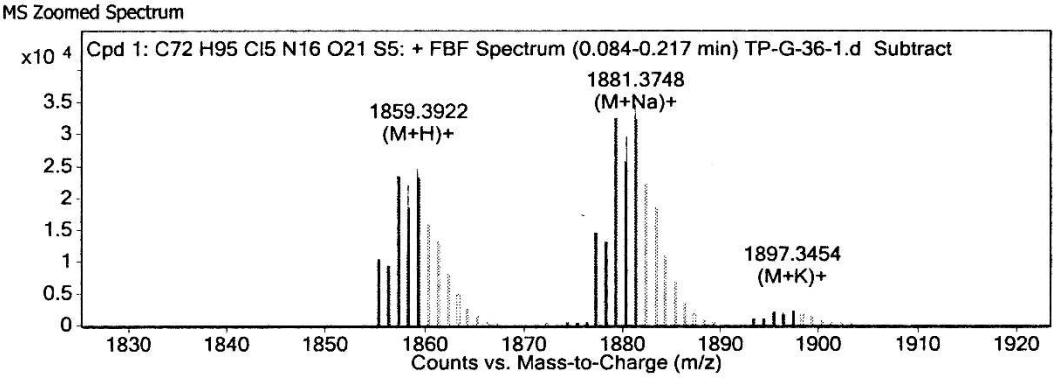

Oligomer **4**

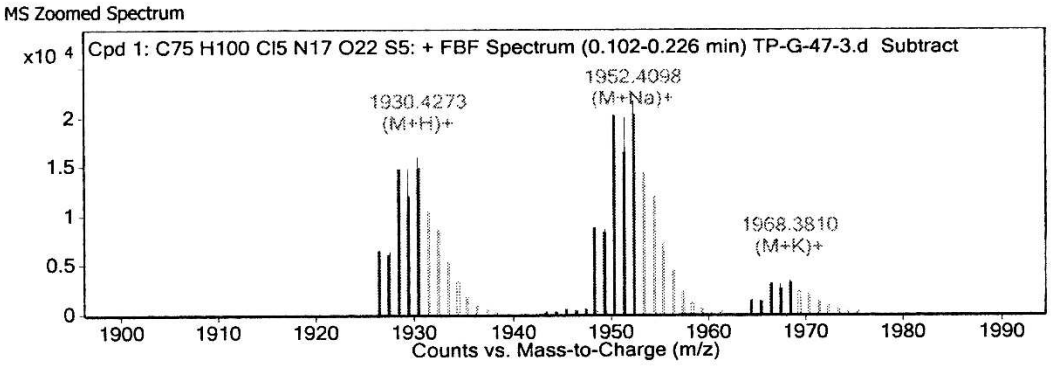

Oligomer **5**

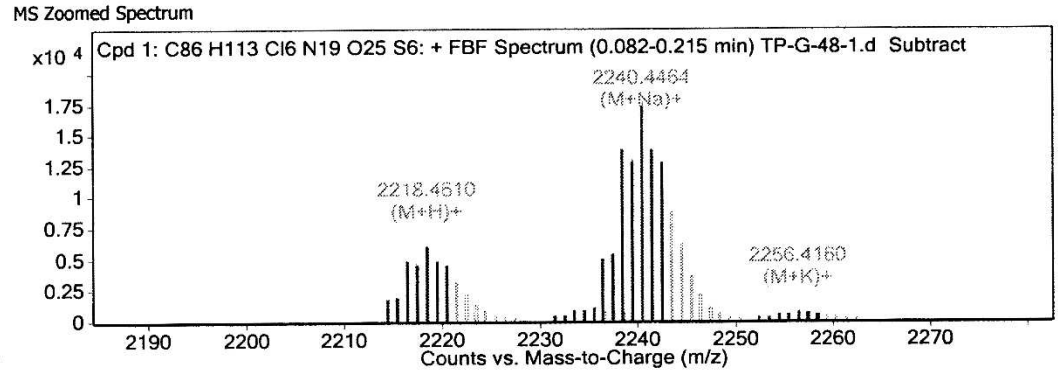

Oligomer **6**

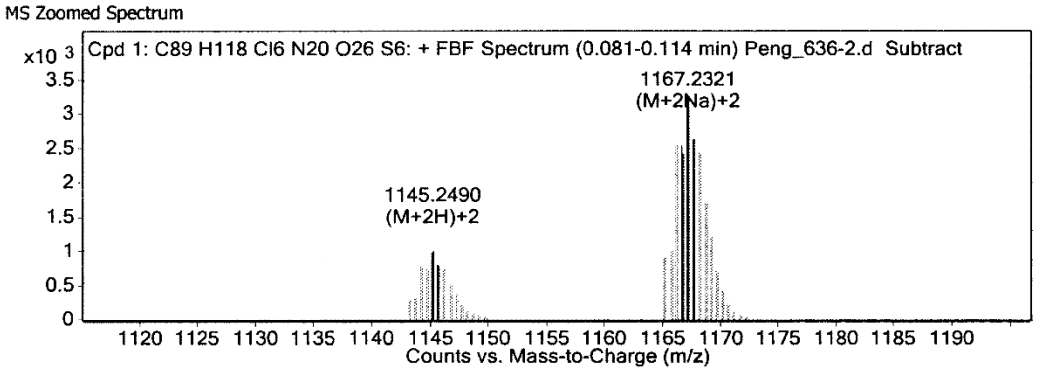

Oligomer 7

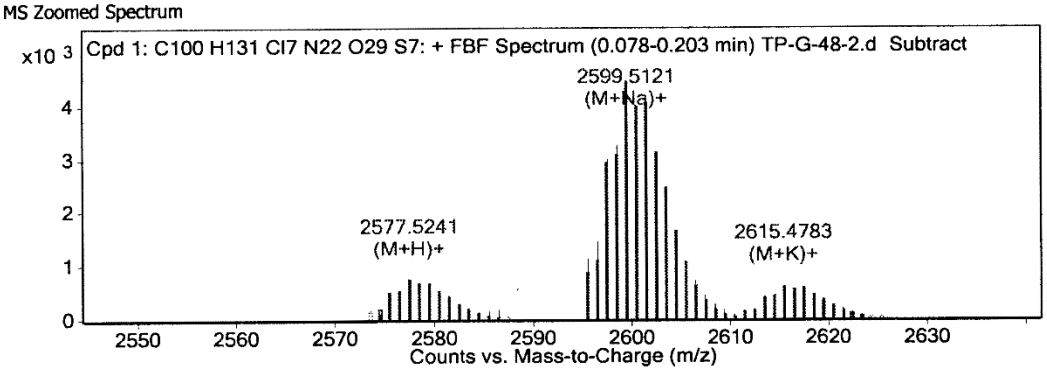

Oligomer 9

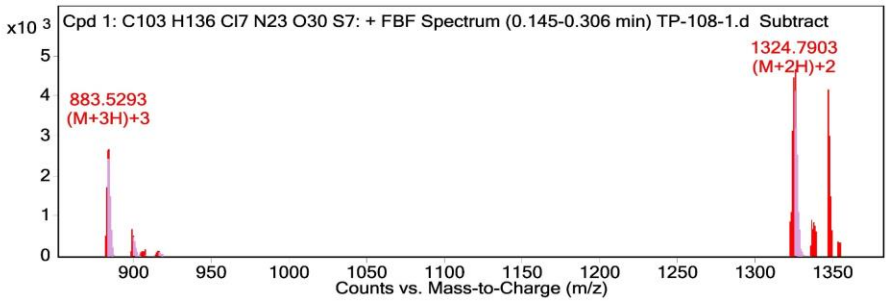

MS Spectrum Peak List

m/z	z	Abund	Formula	Ion
882.1952	3	381.25	C103H139Cl7N23O30S7	(M+3H)+3
898.1774	3	703.99	C103H134Cl7N23Na3O29S7	(M+3Na)+3[-H2O]
904.8322	3	87.29	C103H136Cl7N23Na3O30S7	(M+3Na)+3
914.1518	3	81.25	C103H134Cl7K3N23O29S7	(M+3K)+3[-H2O]
1322.7923	2	608.13	C103H138Cl7N23O30S7	(M+2H)+2
1324.2906	2	3475.52	C103H138Cl7N23O30S7	(M+2H)+2
1324.7903	2	4691.55	C103H138Cl7N23O30S7	(M+2H)+2
1335.78	2	699.87	C103H134Cl7N23Na2O29S7	(M+2Na)+2[-H2O]
1345.763	2	4187.48	C103H136Cl7N23Na2O30S7	(M+2Na)+2
1351.7506	2	368.51	C103H134Cl7K2N23O29S7	(M+2K)+2[-H2O]

Oligomer 10

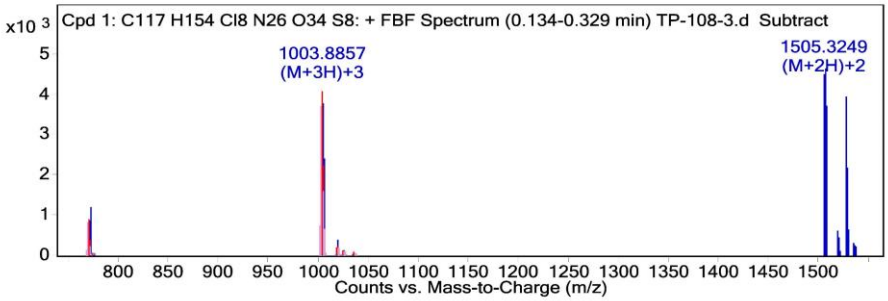

MS Spectrum Peak List

m/z	z	Abund	Formula	Ion
770.6426	4	113.07	C117H152Cl8N26Na4O33S8	(M+4Na)+4[-H2O]
774.8915	4	29.51	C117H154Cl8N26Na4O34S8	(M+4Na)+4
1003.5526	3	3613.13	C117H157Cl8N26O34S8	(M+3H)+3
1018.8664	3	413.37	C117H152Cl8N26Na3O33S8	(M+3Na)+3[-H2O]
1025.1937	3	164.93	C117H154Cl8N26Na3O34S8	(M+3Na)+3
1034.8414	3	89.58	C117H152Cl8K3N26O33S8	(M+3K)+3[-H2O]
1504.8253	2	4518.36	C117H156Cl8N26O34S8	(M+2H)+2
1517.8055	2	633.86	C117H152Cl8N26Na2O33S8	(M+2Na)+2[-H2O]
1525.7979	2	3945.88	C117H154Cl8N26Na2O34S8	(M+2Na)+2
1533.7838	2	328.35	C117H152Cl8K2N26O33S8	(M+2K)+2[-H2O]

Figure S2. HRMS spectra of oligomers **1**–**10**.

2. Crystal packing of compounds 4, 6, and 7

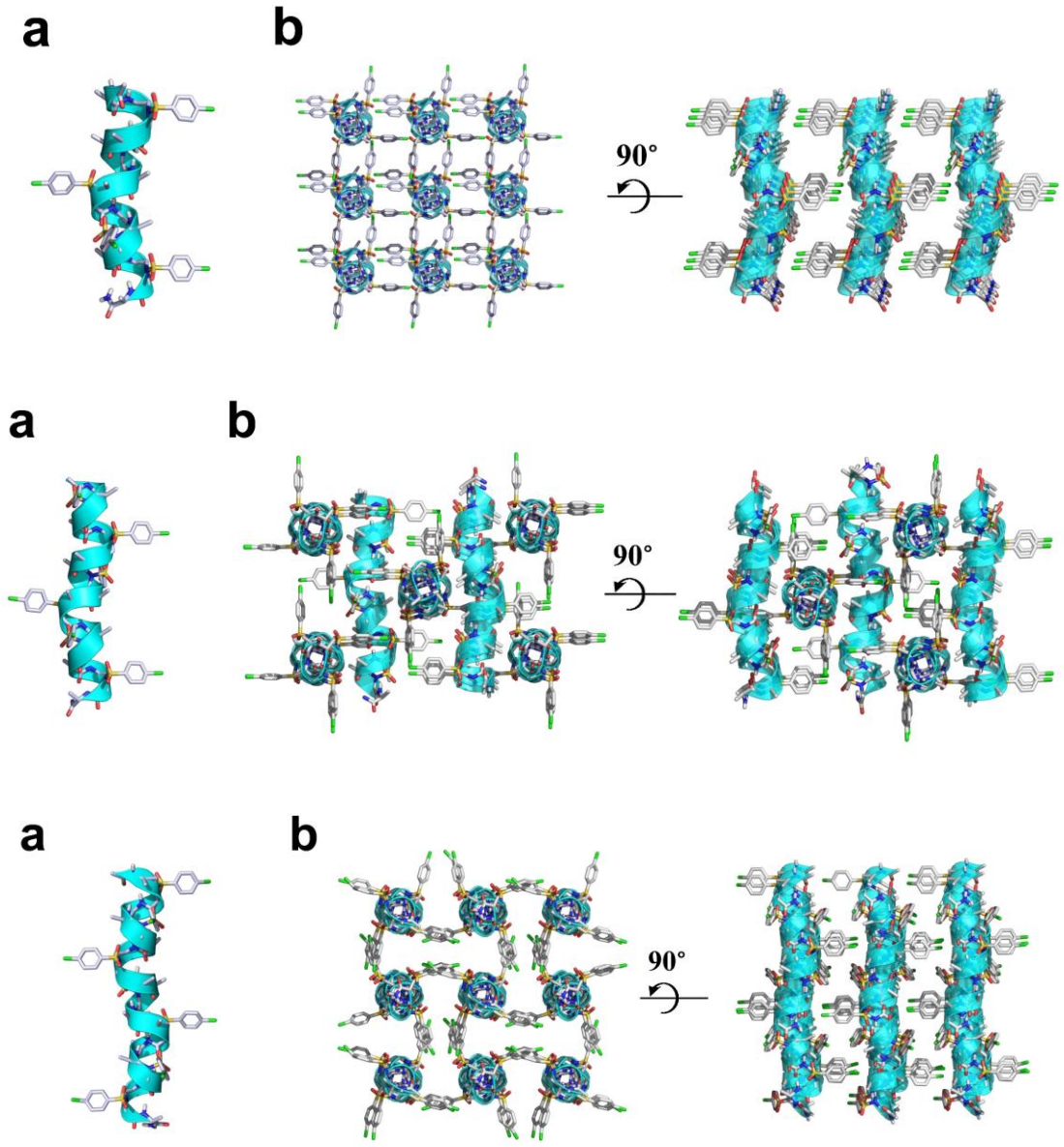

Figure S3. Crystal packing. (a) Helical cartoon representation of **4**, **6**, or **7 B** (from top to bottom) shown as dumbbell. (b) Crystal packing of **4**, **6**, or **7**. Solvent molecules were also excluded from the crystal lattice.

3. NMR studies of oligomer 8

The NMR spectra were obtained on a Varian VNMRS 600 MHz spectrometer equipped with four RF channels and a Z-axis-pulse-field gradient cold probe. Oligomer **8** was dissolved in 0.5 mL of

CD_3OH in a 5 mm NMR tube at a concentration of 4 mM. The ^1H shift assignment was achieved by sequential assignment procedures based on DQFCOSY, COSY, zTOCSY and NOESY measurement. COCSY and NOESY spectra were acquired with the Wet solvent suppression at Varian 600 MHz at 10 ºC. All experiments were performed by collecting 4096 points in f2 and 300 points in f1. A DIPSI2 spin lock sequence with a spin lock field of 6k Hz and mixing time of 80 ms were used in zTOCSY. NOESY experiment was carried out using a mix time of 200 ms. Vnmrj was used to process and analyze 2D NMR data.

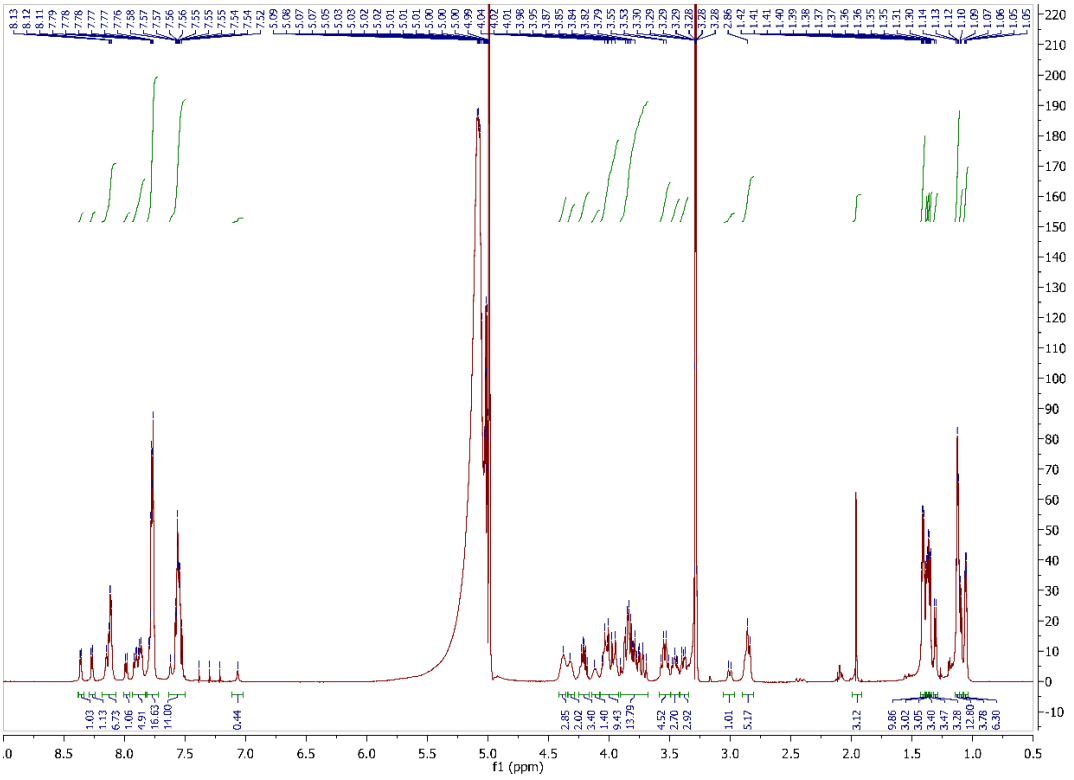

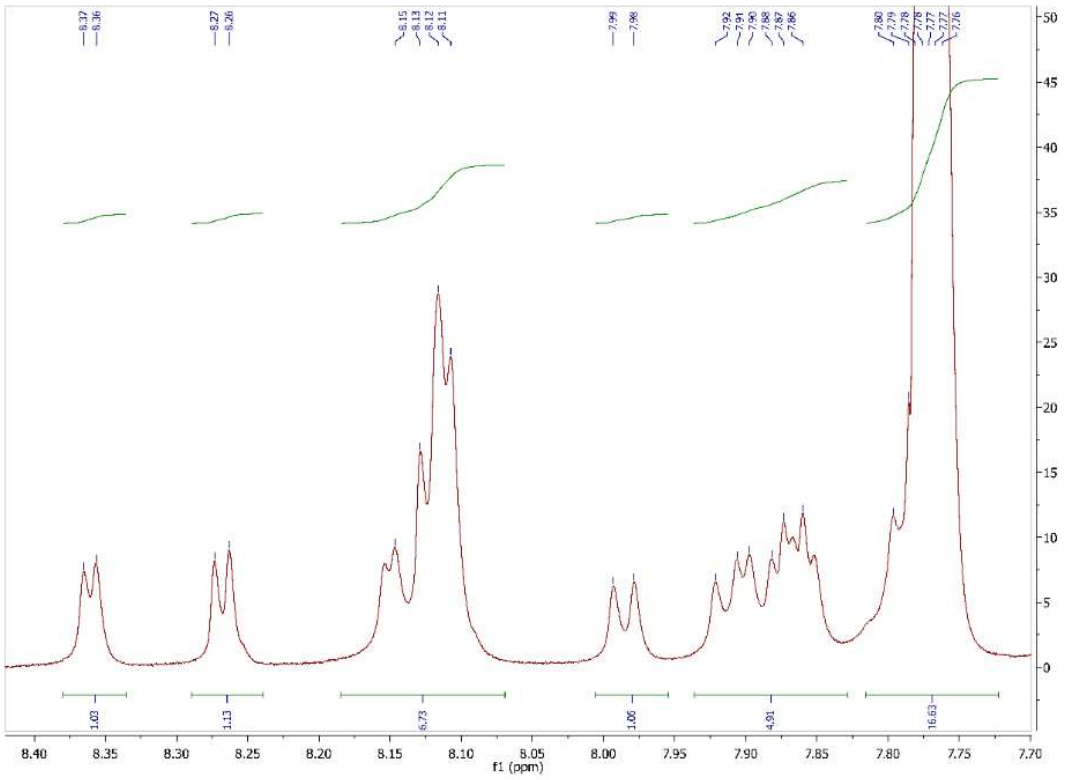
f1 (ppm)

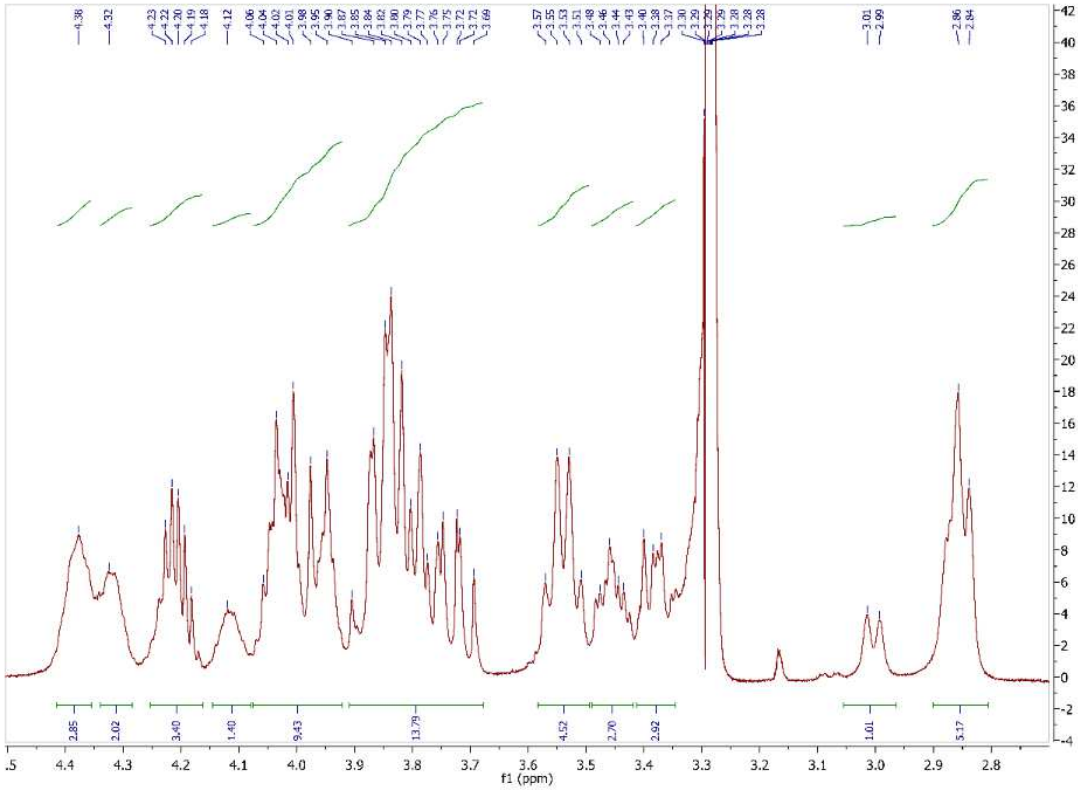
f1 (ppm)

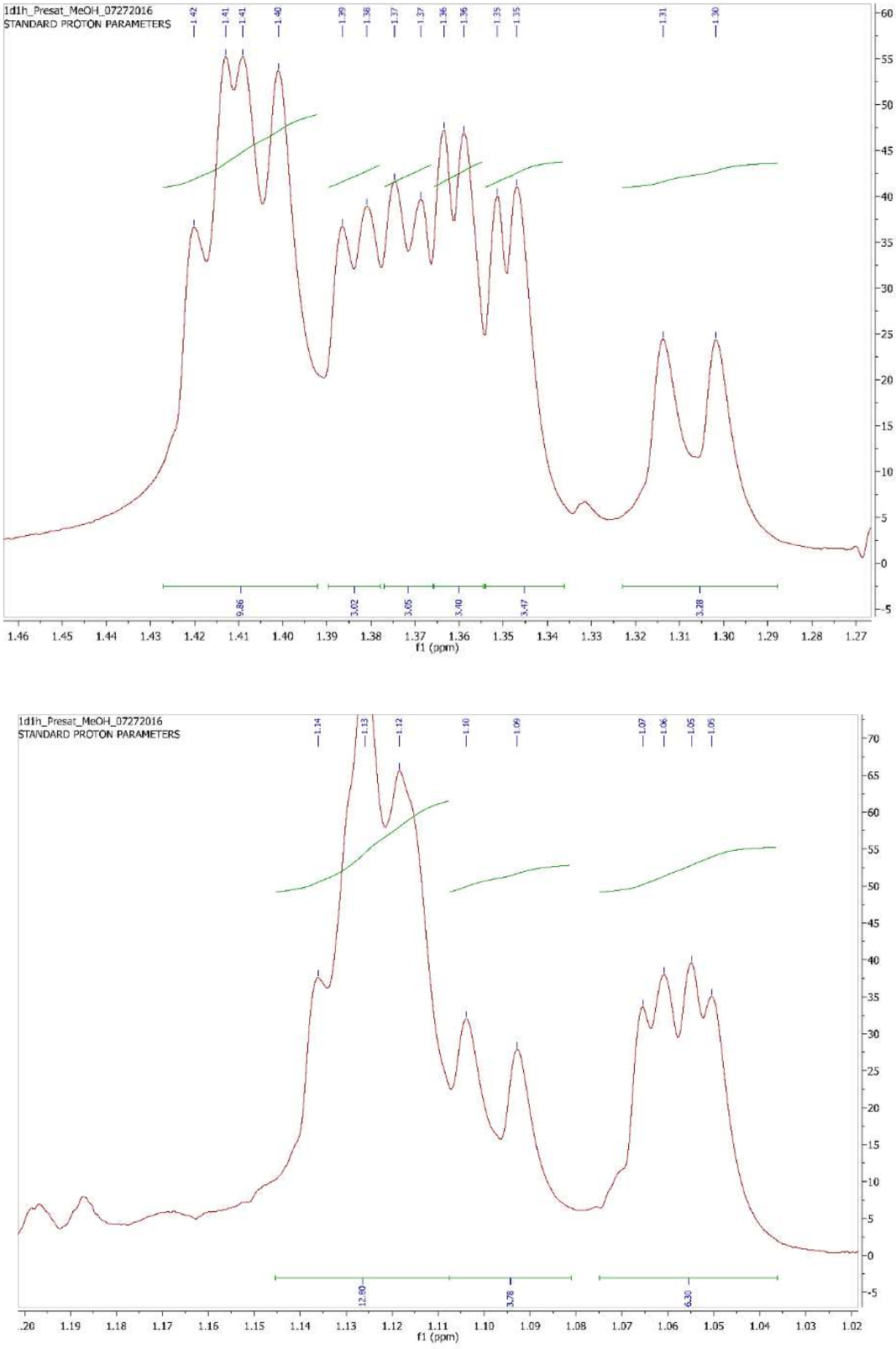

Figure S4. ^{1}H NMR spectra of oligomer **8** in CD_3OH.

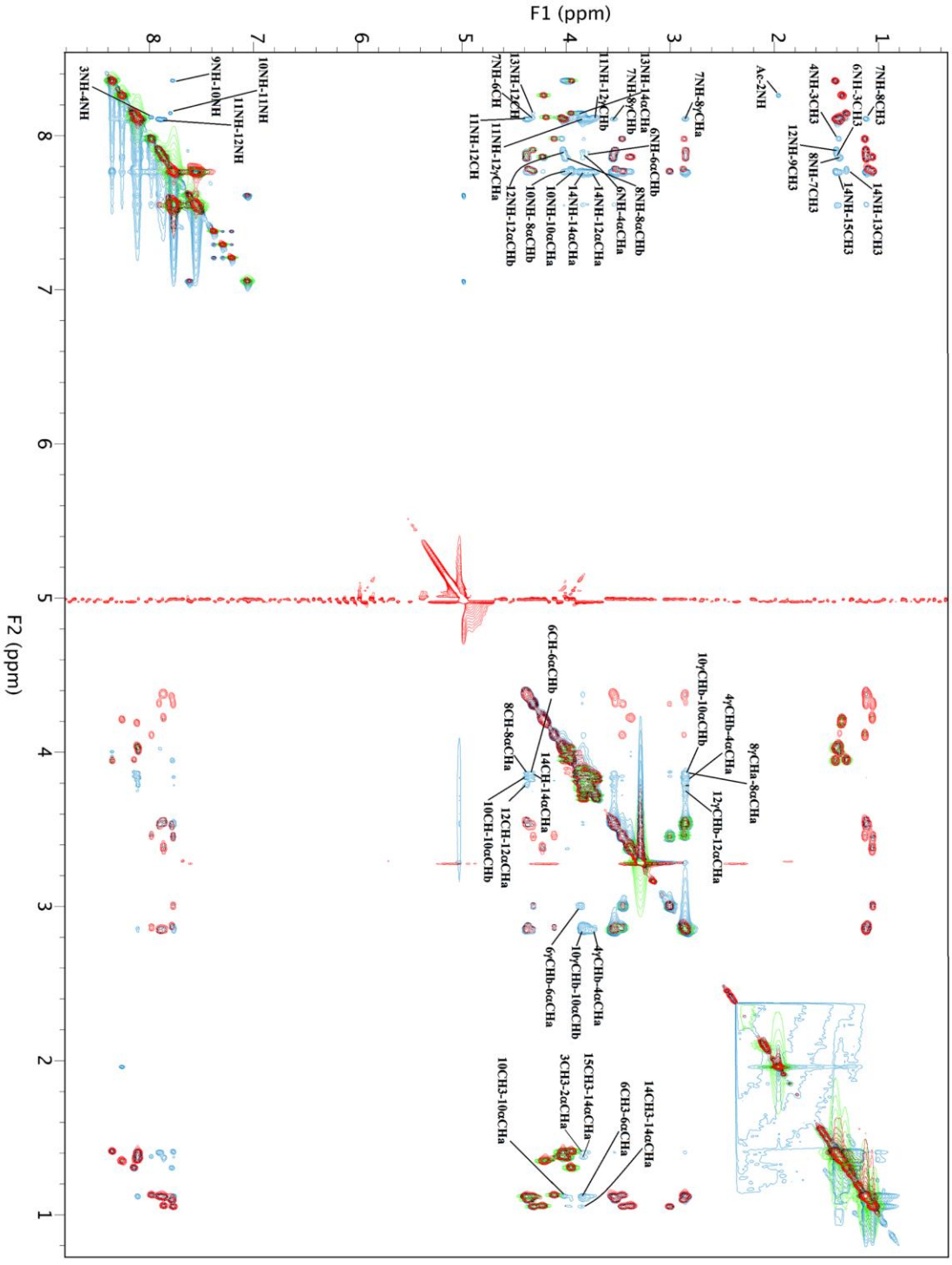
F1 (ppm)
F2 (ppm)
7NH-8CH3
6NH-3CH3
4NH-3CH3
12NH-9CH3
Ac-2NH
14NH-13CH3
14NH-15CH3
8NH-7CH3
7NH-8γCHa
13NH-14αCHa
7NH-8γCHb
11NH-12γCHb
6NH-6αCHb
8NH-8αCHb
6NH-4αCHa
14NH-12αCHa
14NH-14αCHa
10NH-10αCHa
10NH-8αCHb
12NH-12αCHb
13NH-12CH
7NH-6CH
11NH-12CH
11NH-12γCHa
10NH-11NH
9NH-10NH
11NH-12NH
3NH-4NH
8γCHa-8αCHa
4γCHb-4αCHa
10γCHb-10αCHb
12γCHb-12αCHa
6CH-6αCHb
8CH-8αCHa
14CH-14αCHa
12CH-12αCHa
10CH-10αCHb
6γCHb-6αCHa
4γCHb-4αCHa
10γCHb-10αCHb
14CH3-14αCHa
6CH3-6αCHa
15CH3-14αCHa
3CH3-2αCHa
10CH3-10αCHa

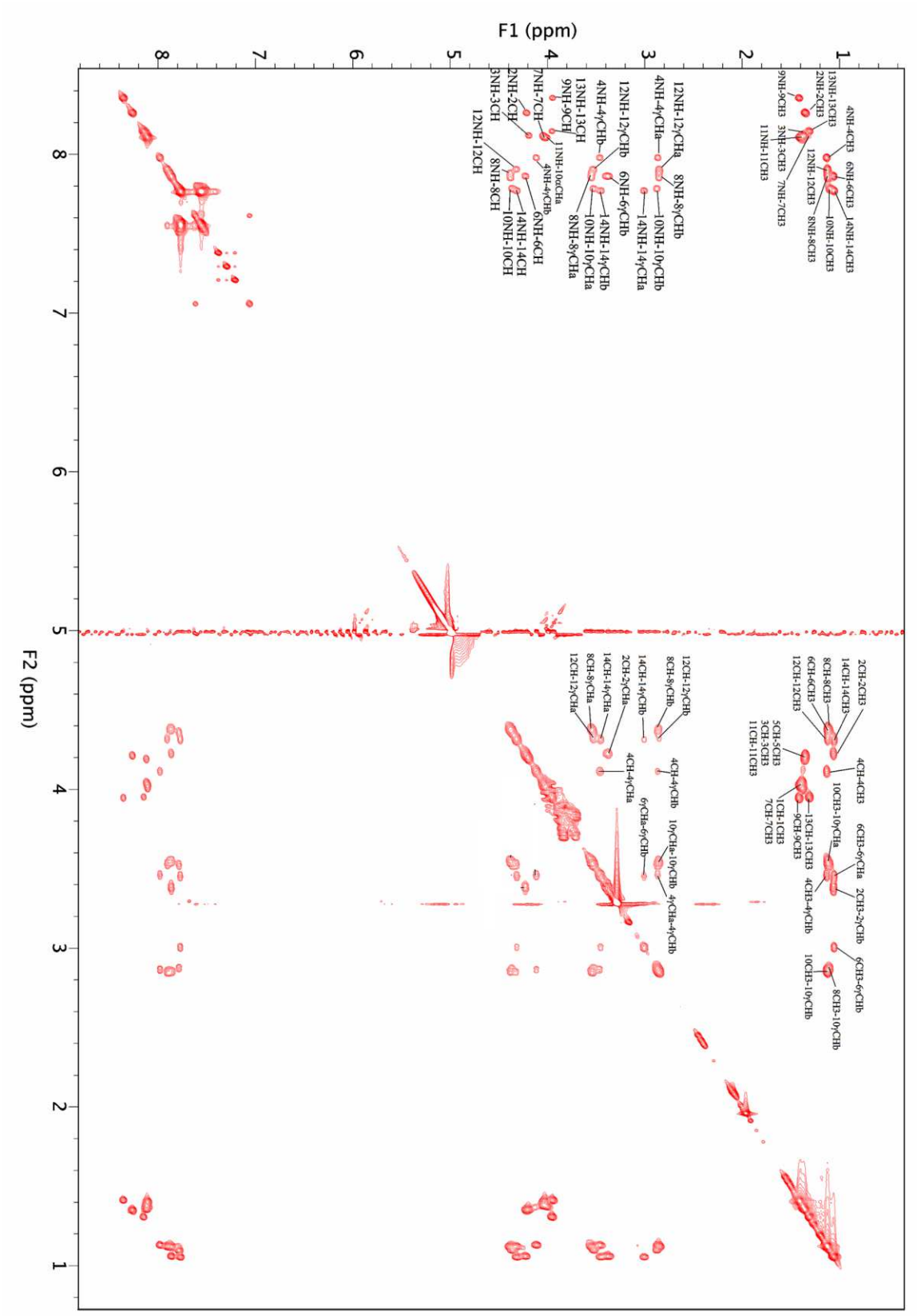
F1 (ppm)
F2 (ppm)
4NH-4CH3
6NH-6CH3
14NH-14CH3
13NH-13CH3
2NH-2CH3
10NH-10CH3
12NH-12CH3
8NH-8CH3
9NH-9CH3
3NH-3CH3
7NH-7CH3
11NH-11CH3
12NH-12γCHa
8NH-8γCHb
4NH-4γCHa
10NH-10γCHb
14NH-14γCHa
12NH-12γCHb
6NH-6γCHb
4NH-4γCHb
14NH-14γCHb
13NH-13CH
10NH-10γCHa
9NH-9CH
8NH-8γCHa
7NH-7CH
11NH-10αCHa
4NH-4γCHb
6NH-6CH
2NH-2CH
14NH-14CH
3NH-3CH
10NH-10CH
12NH-12CH
8NH-8CH
2CH-2CH3
14CH-14CH3
8CH-8CH3
6CH-6CH3
12CH-12CH3
5CH-5CH3
3CH-3CH3
11CH-11CH3
1CH-1CH3
7CH-7CH3
4CH-4CH3
10CH3-10γCHa
9CH-9CH3
13CH-13CH3
6CH3-6γCHa
2CH3-2γCHb
4CH3-4γCHb
6CH3-6γCHb
8CH3-10γCHb
10CH3-10γCHb
12CH-12γCHb
8CH-8γCHb
14CH-14γCHb
4CH-4γCHb
10γCHa-10γCHb
4γCHa-4γCHb
6γCHa-6γCHb
2CH-2γCHa
14CH-14γCHa
8CH-8γCHa
12CH-12γCHa
4CH-4γCHa

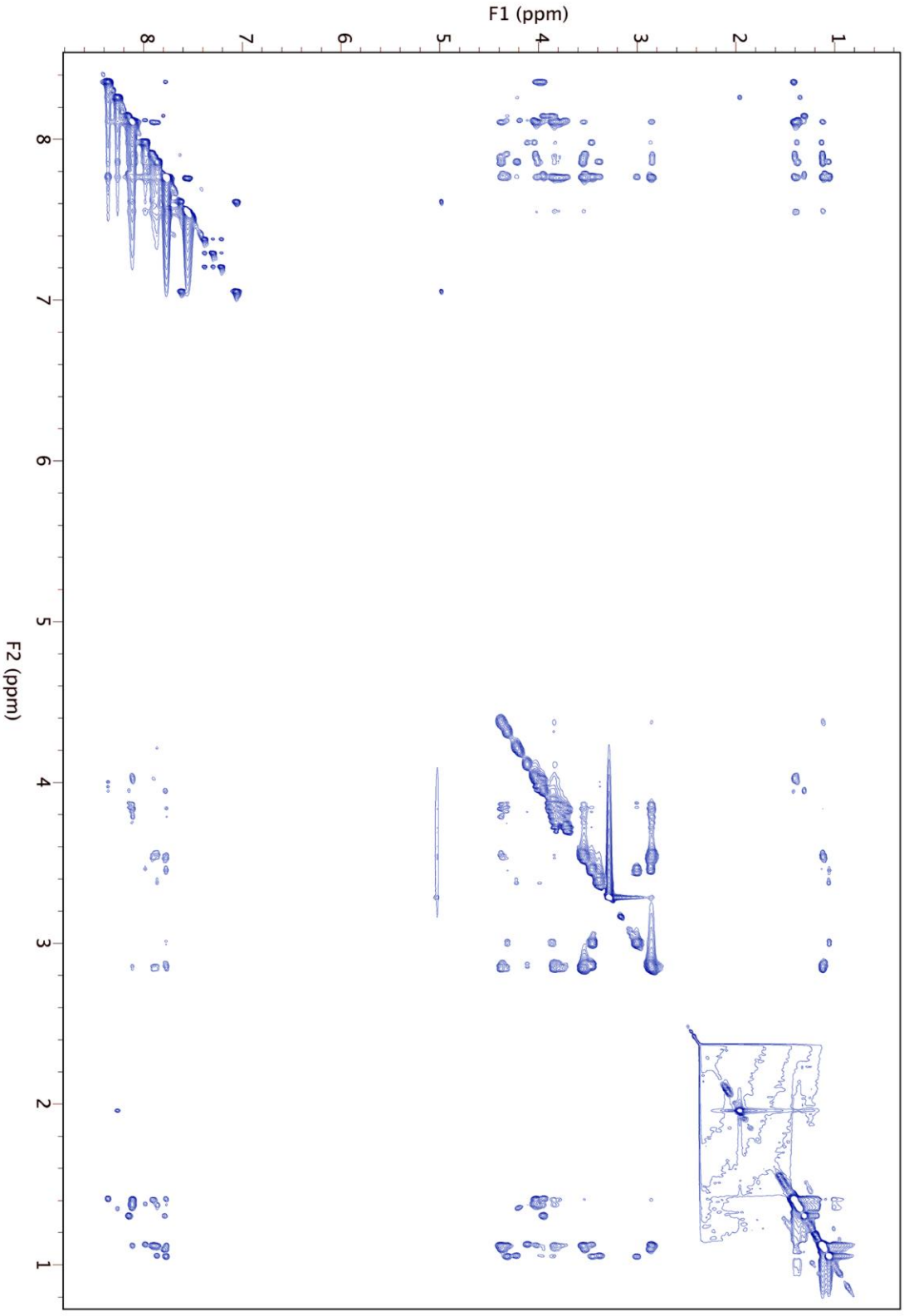
F1 (ppm)
F2 (ppm)

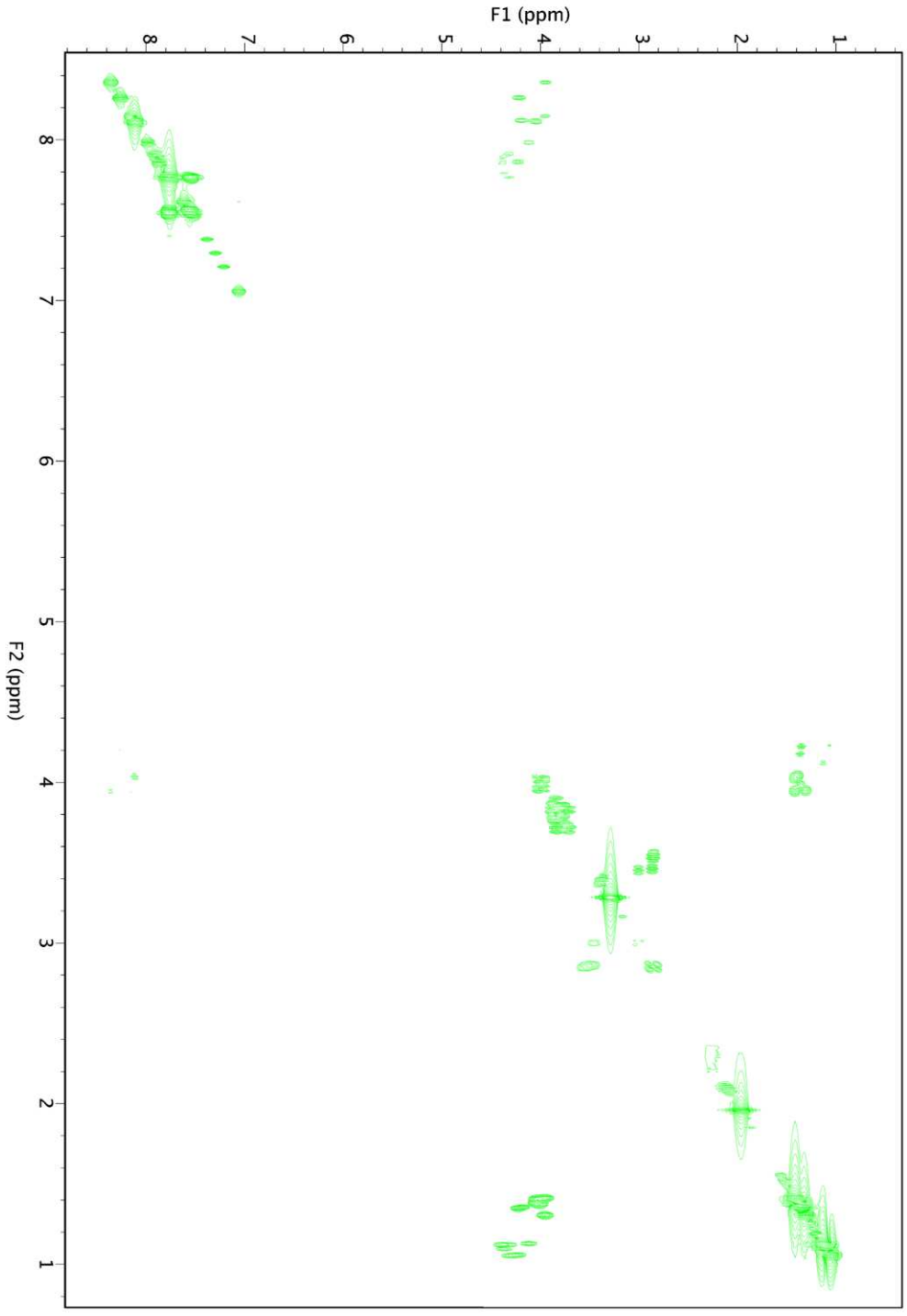

Figure S5. Annotated natural 2D spectra for oligomer **8**. The spectra were collected at 600 MHz at a temperature of 10 ºC. Chemical shift assignments were based on ^{1}H, ^{1}H-zTOCSY (red color), ^{1}H-NOESY (blue color), and ^{1}H-COSY (green color).

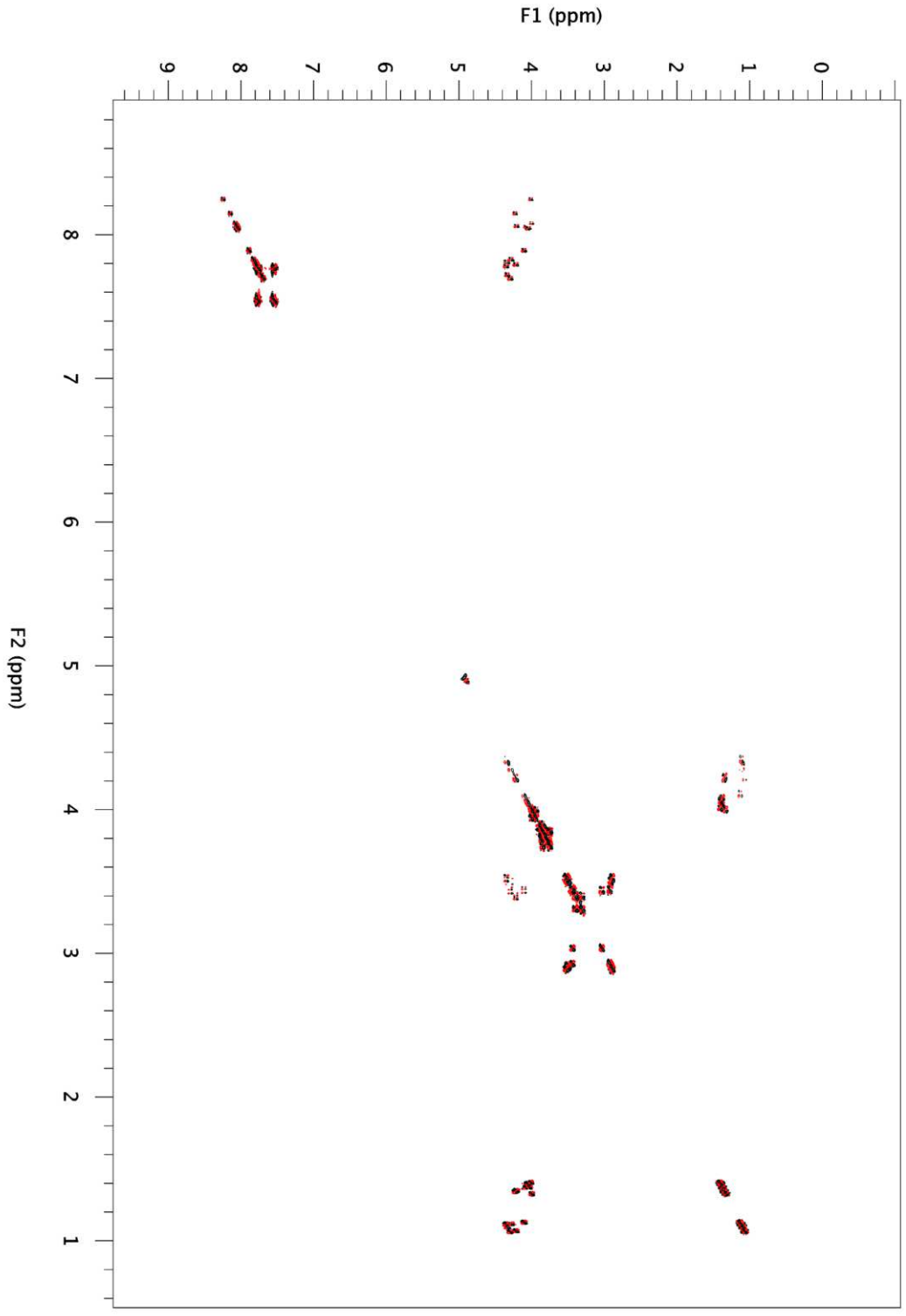

Figure S6. DQFCOSY spectrum for oligomer **8**.

4. X-ray crystallography

Lyophilized powders of oligomers **6** (3 mg), **9** (3 mg) and **10** (2 mg) were dissolved in 2 mL of dichloromethane/acetonitrile (20:80, v/v) and then left for slow evaporation at room temperature within two days to give crystals. Lyophilized powders of oligomers **4** (2 mg) were dissolved in THF (2 mL) and then pentane (1 mL) was diffused slowly into THF layer, crystals were formed in a week. Crystals of **7** were obtained from slow evaporation of 3 mg/mL solution in chloroform. Oligomers **2** was also crystalized from slow diffusion of pentane into THF in ten days, however, the crystals were not of good quality for X-ray diffraction (diffraction up to 5.00 Å of resolution only). Foldamers 8 and 9 in 1:1 ratio (4 mg, the racemate 11) was crystallized from CH2Cl2/CH3CN (60:40, v/v) using slow vaporization over two days.

Both compound **4** and **7** crystallize in $P2_1$ space group with one molecule in the asymmetric unit. While compounds **6** and **8** crystallize in $P4_12_12$ space group with two α peptide and two sulfono-γ-AA peptide residues in the asymmetric unit. In contrast, compounds **9** and **10** crystallize in $P4_32_12$ space group with two α peptide and two sulfono-γ-AA peptide residues in the asymmetric unit. The apparent infinite chain in structures **6**, **9**, and **10** is an effect of translational disorder in those structures and occupancy of atoms in model were adjusted to match the appropriate formulas, therefore the N-terminal acetyl group was not visible.

The X-ray diffraction data for all compounds were measured on Bruker D8 Venture PHOTON 100 CMOS system equipped with a Cu K_α INCOATEC Imus micro-focus source (λ = 1.54178 Å). Indexing was performed using APEX3(*4*) (Difference Vectors method). Data integration and reduction were performed using SaintPlus 6.01(*5*). Absorption correction was performed by multi-scan method implemented in SADABS(*6*). Space groups were determined using XPREP implemented in APEX3. Structures were solved using SHELXT or SHELXD and refined using SHELXL-2014(*7-9*) (full-matrix least-squares on F^2) through OLEX2 interface program(*10*).

For compound **4**, diffraction spots were observed up to ca. 1.1 Å resolution. The structure has been solved using program Shelxd(*11*) and refined using geometry and ADP restraints. Inspection of 2Fo-Fc electron density map in WinCoot(*12*) suggested the THF as disordered solvent. THF was subsequently modeled into the map, real space refined with WinCoot and finally refined with Shelxl with fixed occupancy and restraints. The group of electron density peaks located between aromatic rings of two helices have been tentatively assigned as pyridine and refined with restrains. Crystal data and refinement conditions are shown in Table S3.

Table S2: Crystal data and structure refinement for Oligomer **4**.	
Identification code	PT_G47_3_0422
Empirical formula	$C_{102}H_{149}Cl_5N_{18}O_{27.5}S_5$
Empirical formula	$C_{75}H_{100}Cl_5N_{17}O_{22}S_5 \cdot 5.5THF \cdot C_5H_5N$
Formula weight	2404.93
Temperature/K	100(2)
Crystal system	monoclinic
Space group	$P2_1$
a/Å	12.5708(14)
b/Å	51.249(6)
c/Å	12.9887(14)
α/°	90
β/°	90.116(2)
γ/°	90
Volume/Å^3	8367.8(16)
Z	2
ρ_{calc}g/cm^3	0.954
μ/mm^{-1}	1.835
F(000)	2544.0
Crystal size/mm^3	0.400 × 0.090 × 0.080
Radiation	CuKα (λ = 1.54178)
2Θ range for data collection/°	6.806 to 89.062
Index ranges	$-11 \leq h \leq 11$, $-46 \leq k \leq 46$, $-11 \leq l \leq 11$
Reflections collected	55363
Independent reflections	12960 [R_{int} = 0.0859, R_{sigma} = 0.1006]
Data/restraints/parameters	12960/2258/1403
Goodness-of-fit on F^2	1.254
Final R indexes [I>=2σ (I)]	R_1 = 0.1308, wR_2 = 0.3169
Final R indexes [all data]	R_1 = 0.1839, wR_2 = 0.3451

Largest diff. peak/hole / e $Å^{-3}$	0.55/-0.49
Flack parameter	0.124(8)

For compound **6**, the structure solution has led to apparent "infinite" helix which can be explained through the presence of translational disorder between discrete chains in the crystal. The occupancy of each of two C3NSO2PhCl parts (of sulfono-γ-AApeptide) has been adjusted to 0.857 in asymmetric unit to match the ratio of alanine to sulfono-γ-AApeptide (7:6). From the disorder point of view when C3NSO2PhCl part is missing the terminal part of peptide is present leading to the column formed out of peptide helices interacting through hydrogen bonds. The disordered Ph-Cl groups and solvent (CH_3CN) have been refined using restraints. Crystal data and refinement conditions are shown in Table S4.

Table S3: Crystal data and structure refinement for oligomer **6.**	
Identification code	pt_g_36_2_0m
Empirical formula	$C_{106.5}H_{144.25}Cl_6N_{28.75}O_{26}S_6$
Moiety Formula	$C_{89}H_{118}Cl_6N_{20}O_{26}S_6$, $8.75CH_3CN$
Formula weight	2648.18
Temperature/K	100(2)
Crystal system	tetragonal
Space group	$P4_12_12$
a/Å	17.1537(4)
b/Å	17.1537(4)
c/Å	28.9825(8)
α/°	90
β/°	90
γ/°	90
Volume/$Å^3$	8528.1(5)
Z	2.29
$\rho_{calc}g/cm^3$	1.179
μ/mm^{-1}	2.406
F(000)	3178.0
Crystal size/mm^3	0.140 × 0.140 × 0.120
Radiation	CuKα (λ = 1.54178)
2Θ range for data collection/°	7.288 to 138.224
Index ranges	$-20 \leq h \leq 20$, $-20 \leq k \leq 20$, $-34 \leq l \leq 32$
Reflections collected	64938
Independent reflections	7920 [R_{int} = 0.0514, R_{sigma} = 0.0337]

Data/restraints/parameters	7920/128/503
Goodness-of-fit on F^2	1.081
Final R indexes [I>=2σ (I)]	R_1 = 0.0957, wR_2 = 0.2648
Final R indexes [all data]	R_1 = 0.1275, wR_2 = 0.3132
Largest diff. peak/hole / e $Å^{-3}$	0.46/-0.36
Flack parameter	0.040(9)

For compound **7**, Diffraction spots were observed only up to ca. 1.2 – 1.30 Å resolution. The structure has been solved using program Shelxd (*11*) using NSO2 fragment seeding and completed using Fourier methods in Shelxl. Due to low resolution and disorder, restraints were necessary to refine positions and anisotropic thermal parameters. The model of the crystal structure has been refined as pseudo merohedral twin (TWIN 1 0 0 0 -1 0 0 0 -1 2). After each refinement run the 2Fo-Fc map has been inspected using Program WinCoot, especially for significantly disordered terminal residues, to assure that atoms are located within the map contours (at 0.6–1 sigma level). Distances of O…N hydrogen bonds were restrained at terminal sides to prevent drifting of disordered residues. The disordered chloroform molecules have been refined using restraints. The inspection of 2Fo-Fc electron density map in WinCoot had clearly suggested the $CHCl_3$ as disordered solvent. $CHCl_3$ was subsequently modeled into the map, real space refined with WinCoot and finally refined with Shelxl with fixed occupancy and restraints. Some of the larger residual electron density peaks have been tentatively assigned as Cl with assumption they are a part of heavily disordered chloroform molecules that could not be easily localized. The relatively high R-factor is caused mostly by unaccounted disordered solvent molecules – it can be lowered to ~11% through application of Squeeze solvent mask procedure. This however eliminates chloroform molecules which are important part of crystal packing so solvent corrected data have not been presented for publication. Although the data quality is low per small molecule crystallography standards the main goal of structural analysis was to establish secondary structure, for which purpose the data quality is sufficient in authors' opinion. Crystal data and refinement conditions are shown in Table S5.

Table S4: Crystal data and structure refinement for oligomer **7.**	
Identification code	TP48_2_0m
Empirical formula	$C_{108.83}H_{139.83}Cl_{33.5}N_{22}O_{29}S_7$
Moiety formula	$C_{100}H_{131}Cl_7N_{22}O_{29}S_7 \cdot 8.83CHCl_3$
Formula weight	3632.20
Temperature/K	100(2)
Crystal system	monoclinic
Space group	$P2_1$
a/Å	17.1947(15)
b/Å	17.2126(16)
c/Å	35.063(3)
α/°	90
β/°	90.043(4)
γ/°	90
Volume/Å^3	10377.5(16)
Z	2
ρ_{calc}g/cm^3	1.162
μ/mm^{-1}	5.133
F(000)	3721.0
Crystal size/mm^3	0.120 × 0.100 × 0.060
Radiation	CuKα (λ = 1.54178)
2Θ range for data collection/°	5.134 to 76.15
Index ranges	$-13 \leq h \leq 13$, $-13 \leq k \leq 13$, $-28 \leq l \leq 26$
Reflections collected	20310
Independent reflections	9948 [R_{int} = 0.1247, R_{sigma} = 0.1706]
Data/restraints/parameters	9948/3723/1848
Goodness-of-fit on F^2	1.904
Final R indexes [I>=2σ (I)]	R_1 = 0.2096, wR_2 = 0.4451
Final R indexes [all data]	R_1 = 0.3169, wR_2 = 0.5270
Largest diff. peak/hole / e Å^{-3}	1.04/-0.77
Flack parameter	0.14(2)

Oligomers **9**, **10**, and **11** diffracted up to 0.95 Å resolution. Disordered parts were refined using restraints. Data processing and structure solution of all structures have initially led to apparent "infinite" polymeric" helix and structure with unit cell parameters along the axis of helix shorter than the length of actual helix. This could be explained as an effect of translational disorder between

discrete peptide chains in the crystal as already discussed in previous publication.(*1*) The possible explanation is that discrete peptide chains interact through hydrogen bonds at terminal points to form a "column". Adjacent "Columns" (helices) are interacting weekly. Because seven (or eight) γ-peptide residues are present in single helix, several packing modes are possible, with adjacent helices translated or translated and rotated so that the same weak stabilizing interactions are still present. This leads to translational disorder and diffraction pattern resembling the one from hypothetical structure with "infinite-like" polymeric peptide chains. In reality, the C3NSO2Ph part of the apparent infinite chain is missing at sites where every 8th (or 9th) γ-peptide residue would reside in hypothetical infinite helix. The gap is where hydrogen bond interactions between terminal parts of polypeptides take place. This is accounted for in the model by lower than one occupancy of corresponding part of γ-peptide. The contribution of disordered content in structural voids was treated as diffuse using Squeeze procedure implemented in Platon program.(*13, 14*) Crystal data and refinement conditions are shown in Tables S6-S8.

Table S5. Crystal data and structure refinement for oligomer **9.**	
Identification code	JC_TP_H_108_1
Empirical formula	$C_{103}H_{136}Cl_7N_{23}O_{30}S_7$
Formula weight	2648.91
Temperature/K	99.99
Crystal system	tetragonal
Space group	$P4_32_12$
a/Å	17.1371(4)
b/Å	17.1371(4)
c/Å	29.0104(8)
α/°	90
β/°	90
γ/°	90
Volume/Å^3	8519.8(5)
Z	2
ρ_{calc}g/cm^3	1.033
μ/mm^{-1}	2.369
F(000)	2772.0
Crystal size/mm^3	0.33 × 0.15 × 0.13

Radiation	CuKα (λ = 1.54178)
2Θ range for data collection/°	7.294 to 149.614
Index ranges	$-20 \leq h \leq 21$, $-19 \leq k \leq 16$, $-34 \leq l \leq 36$
Reflections collected	74789
Independent reflections	8717 [R_{int} = 0.0492, R_{sigma} = 0.0328]
Data/restraints/parameters	8717/96/419
Goodness-of-fit on F^2	1.069
Final R indexes [I>=2σ (I)]	R_1 = 0.0661, wR_2 = 0.2052
Final R indexes [all data]	R_1 = 0.0755, wR_2 = 0.2183
Largest diff. peak/hole / e $Å^{-3}$	0.32/-0.29
Flack parameter	0.143(8)

Table S6. Crystal data and structure refinement for oligomer **10.**	
Identification code	TP_H_108_3
Empirical formula	$C_{208}H_{273.78}Cl_{14.22}N_{46.22}O_{60.44}S_{14.22}$
Moiety formula	$1.77779(C_{117}H_{154}Cl_8N_{26}O_{34}S_8)$
Formula weight	5348.61
Temperature/K	99.98
Crystal system	tetragonal
Space group	$P4_32_12$
a/Å	17.1367(3)
b/Å	17.1367(3)
c/Å	28.9848(11)
α/°	90
β/°	90
γ/°	90
Volume/$Å^3$	8511.9(4)
Z	1
$\rho_{calc}g/cm^3$	1.043
μ/mm^{-1}	2.404
F(000)	2798.0
Crystal size/mm^3	0.37 × 0.11 × 0.09
Radiation	CuKα (λ = 1.54178)
2Θ range for data collection/°	5.992 to 108.528
Index ranges	$-18 \leq h \leq 18$, $-18 \leq k \leq 18$, $-28 \leq l \leq 30$
Reflections collected	69116
Independent reflections	5205 [R_{int} = 0.1112, R_{sigma} = 0.0373]

Data/restraints/parameters	5205/204/419
Goodness-of-fit on F^2	1.044
Final R indexes [I>=2σ (I)]	R_1 = 0.0645, wR_2 = 0.1718
Final R indexes [all data]	R_1 = 0.1012, wR_2 = 0.2002
Largest diff. peak/hole / e $Å^{-3}$	0.17/-0.19
Flack parameter	0.045(11)

Table S7. Crystal data and structure refinement for oligomer **11.**	
Identification code	TP_7_MIX
Empirical formula	$C_{103}H_{136}Cl_7N_{23}O_{30}S_7$
Formula weight	2648.91
Temperature/K	150.0
Crystal system	tetragonal
Space group	$I4_1/a$
a/Å	21.1606(12)
b/Å	21.1606(12)
c/Å	17.5048(11)
α/°	90
β/°	90
γ/°	90
Volume/$Å^3$	7838.1(10)
Z	2
ρ_{calc}g/cm^3	1.122
μ/mm^{-1}	2.575
F(000)	2772.0
Crystal size/mm^3	0.3 × 0.28 × 0.25
Radiation	CuKα (λ = 1.54178)
2Θ range for data collection/°	6.552 to 109.012
Index ranges	$-22 \leq h \leq 20$, $-20 \leq k \leq 19$, $-18 \leq l \leq 18$
Reflections collected	19991
Independent reflections	2411 [R_{int} = 0.0670, R_{sigma} = 0.0432]
Data/restraints/parameters	2411/102/210
Goodness-of-fit on F^2	1.119
Final R indexes [I>=2σ (I)]	R_1 = 0.0891, wR_2 = 0.2974
Final R indexes [all data]	R_1 = 0.1074, wR_2 = 0.3173
Largest diff. peak/hole / e $Å^{-3}$	0.26/-0.29

Table S8. Crystal pictures of oligomers **2**, **4**, **6**, **7**, **9**, **10**, and **11**.

Number	Crystal pictures
Oligomer **2**	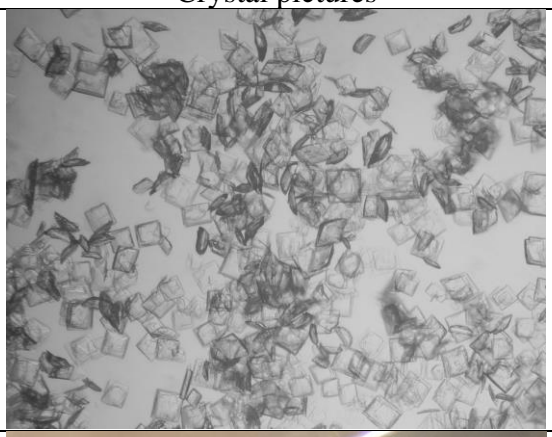
Oligomer **4**	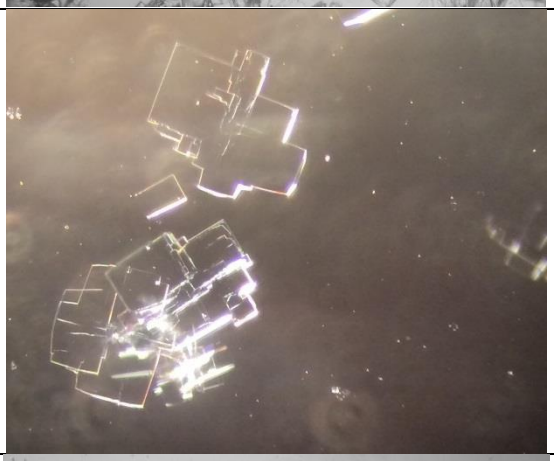
Oligomer **6**	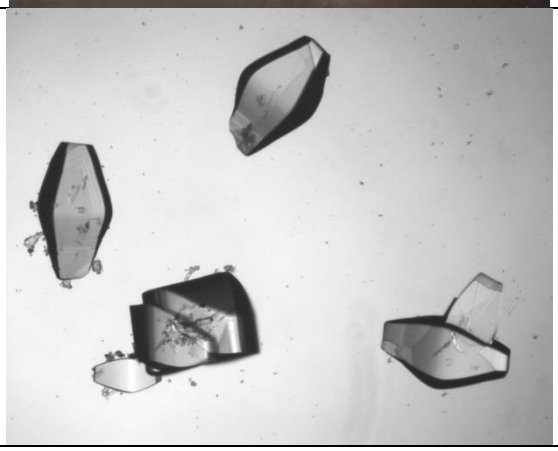

Oligomer **7**		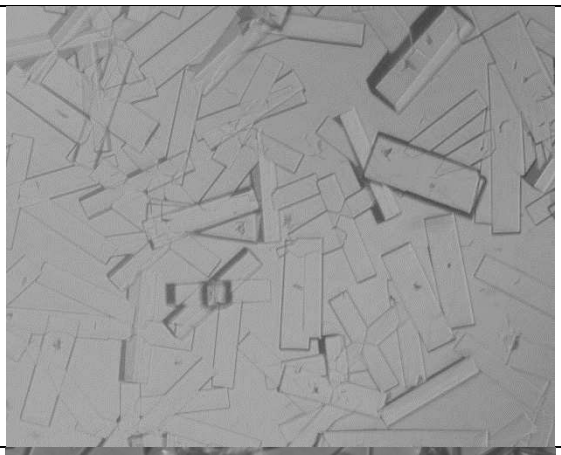	
Oligomer **9**		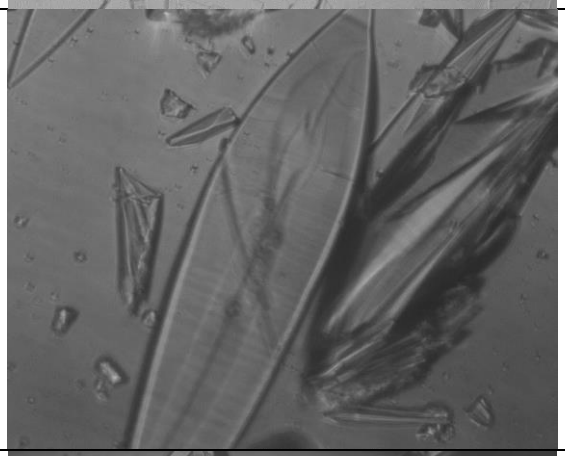	
Oligomer **10**		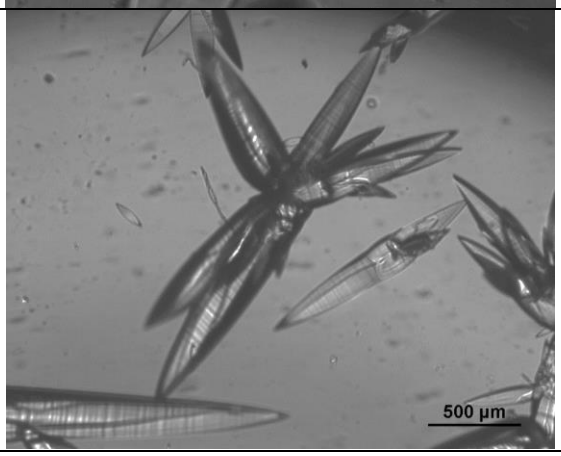	

Racemate **11**		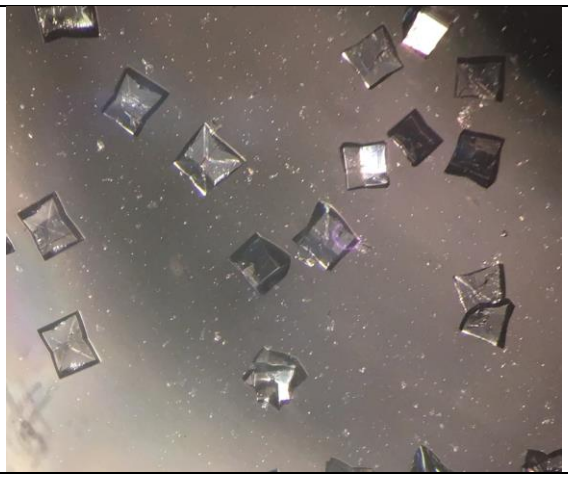

5. Circular dichroism

Circular Dichroism (CD) spectra were measured on an Aviv 215 circular dichroism spectrometer using a 1 mm path length quartz cuvettes, and compound solutions in methanol were prepared using dry weight of the lyophilized solid followed by dilution to give the desired concentrations and solvent combination. 10 scans were averaged for each sample, and 3 times of independent experiments were carried out and the spectra were averaged. The final spectra were normalized by subtracting the average blank spectra. Molar ellipticity [θ] (deg.cm^2.dmol^{-1}) was calculated using the equation:

$[\theta] = \theta_{obs}/(n \times l \times c \times 10)$

Where θ_{obs} is the measured ellipticity in millidegrees, while n is the number of side groups, l is path length in centimeter (0.1 cm), and c is the concentration of the α/sulfono-γ-AA peptide in molar units.

References

1. P. Teng *et al.*, Hydrogen-Bonding-Driven 3D Supramolecular Assembly of Peptidomimetic Zipper. *J. Am. Chem. Soc.* **140**, 5661−5665 (2018).
2. P. Teng *et al.*, Right-Handed Helical Foldamers Consisting of De Novo d-AApeptides. *J. Am. Chem. Soc.* **139**, 7363−7369 (2017).
3. H. Wu *et al.*, New Class of Heterogeneous Helical Peptidomimetics. *Org. Lett.* **17**, 3524−3527 (2015).
4. Bruker (2016). APEX3 (Version 2015.9). Bruker AXS Inc., Madison, Wisconsin, USA.
5. Bruker (2016) SAINT V8.35A. Data Reduction Software.
6. Sheldrick, G. M. (1996). SADABS. Program for Empirical Absorption Correction. University of Gottingen, Germany.
7. Sheldrick, G.M. (1997) SHELXL-97. Program for the Refinement of Crystal.
8. G. Sheldrick, Phase annealing in SHELX-90: direct methods for larger structures. *Acta Cryst. A* **46**, 467−473 (1990).
9. G. Sheldrick, A short history of SHELX. *Acta Cryst. A* **64**, 112−122 (2008).
10. O. V. Dolomanov, L. J. Bourhis, R. J. Gildea, J. A. K. Howard, H. Puschmann, OLEX2: a complete structure solution, refinement and analysis program. *J. Appl. Crystallogr.* **42**, 339−341 (2009).
11. G. Sheldrick, Experimental phasing with SHELXC/D/E: combining chain tracing with density modification. *Acta Cryst. Section D* **66**, 479−485 (2010).
12. P. Emsley, B. Lohkamp, W. G. Scott, K. Cowtan, Features and development of Coot. *Acta Cryst. Section D* **66**, 486−501 (2010).
13. A. Spek, Structure validation in chemical crystallography. *Acta Cryst. D* **65**, 148−155 (2009).
14. R. W. W. Hooft, L. H. Straver, A. L. Spek, Determination of absolute structure using Bayesian statistics on Bijvoet differences. *J. Appl. Crystallogr.* **41**, 96−103 (2008).

Figures

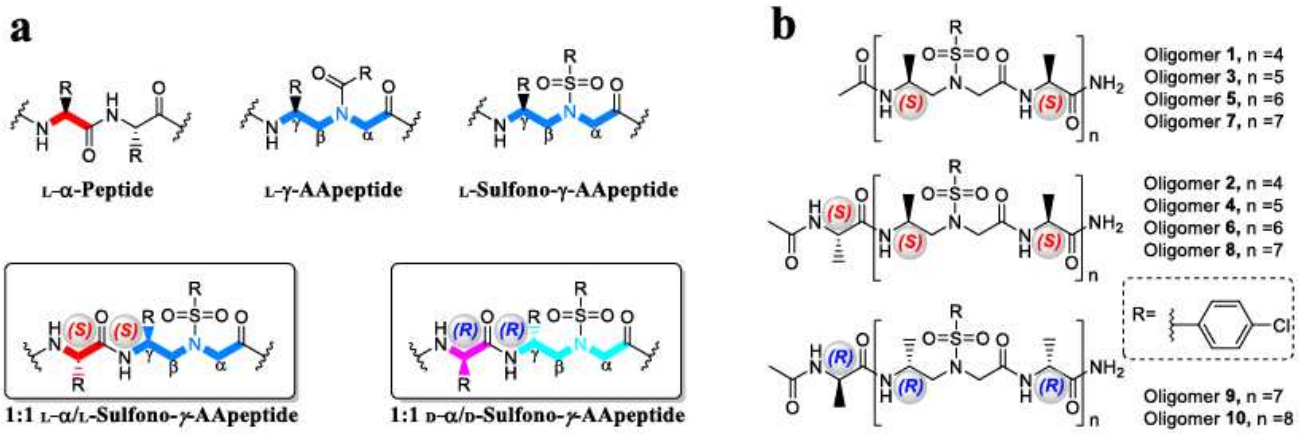

Figure 1

Chemical structures. (A) General structures of L-α-peptides, L-γ-AApeptides, L-sulfono-γ-AApeptides, 1:1 L-α/L-sulfono-γ-AApeptides, and 1:1 D-α/D-sulfono-γ- AApeptides. (B) 1:1 oligomer evaluated in the current study, both the exact ratio of 1:1 (1, 3, 5, and 7) and 1: 1+α (2, 4, 6, 8, 9 and 10) types of oligomers were included.

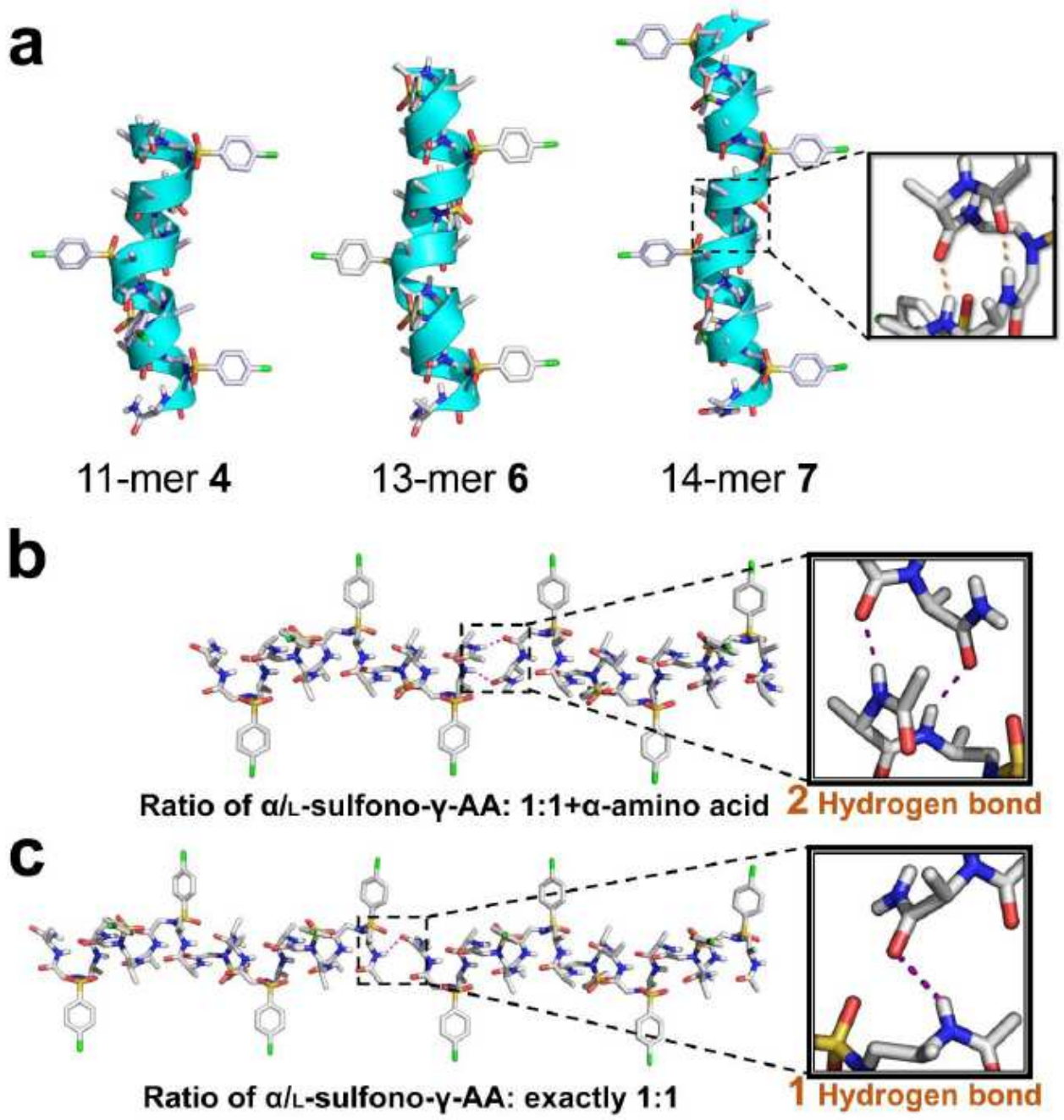

Figure 2

Single crystal structures (a) Single-crystal structures of 413-helix formed by 11-mer 4, 13-mer 6, and 14-mer 7. The intramolecular hydrogen bond was indicated as orange dashed line in the inset. The nonpolar hydrogens were omitted for clarity. Solvent molecules were also excluded from the crystal lattice. (b) Two sets of head-to-tail intermolecular hydrogen bonding in the 1:1+α type of oligomers; (c) One set of head-to-tail intermolecular hydrogen bonding in the exactly 1:1 ratio type of oligomers. (d) A comparison of π-helix and 413-helix. Left: a short seven residue π-helix (orange) embedded within a longer α-helix (green),

taken from PDB code 3QHB. Right: a short seven residue fragment of π-helix mimetic (orange), taken from 11-mer 4.

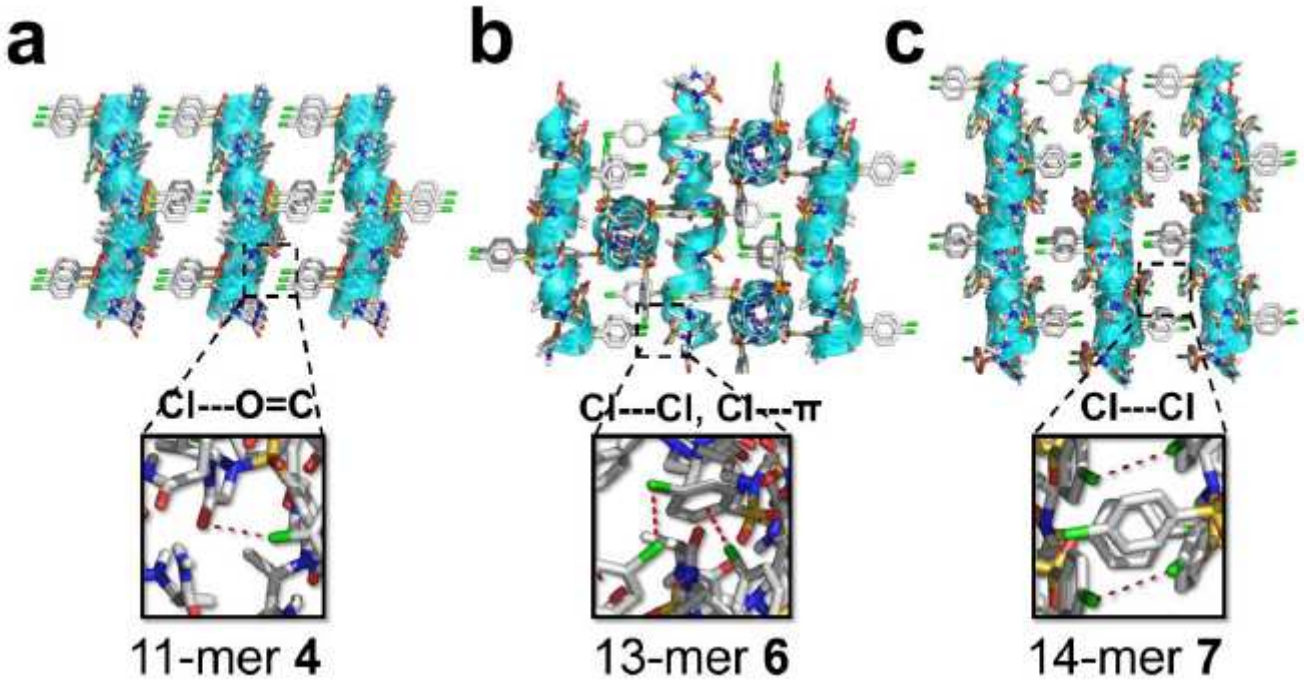

Figure 3

Crystal packing of foldamers. (a) Crystal packing of 11-mer 4. (b) Crystal packing of 13-mer 6. (c) Crystal packing of 14-mer 7. The intermolecular Cl···O=C, C–Cl···Cl–C, and C–Cl···π interactions are indicated as red dashed line in insets.

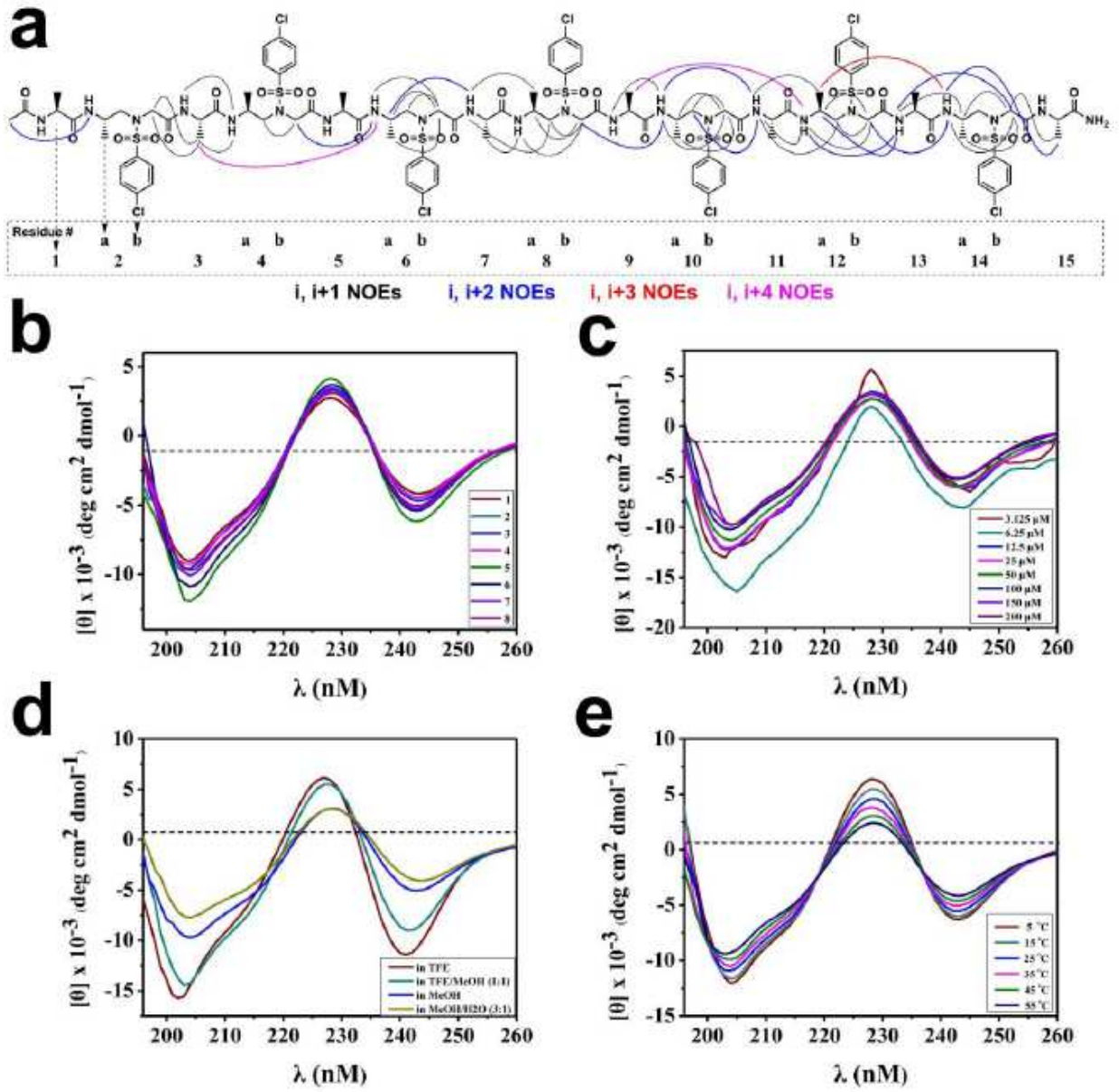

Figure 4

Solution structures of foldamers. (a) Summary of detected NOESY cross-peaks (200 ms mixing time) of foldamer 8 between protons on nonadjacent residues in CD3OH (4 mM concentration, 10 oC). Four types of NOEs are displayed in different color. Each L-sulfono-γ-AA peptide unit is considered as two residues since it is equal to two α-amino acids in length. (b) CD spectra of compounds 1–8 (100 μM) measured at room temperature in CH3OH. (c) CD spectra of compound 8 in CH3OH at various concentrations at room temperature. (d) CD spectra of compound 8 (100 μM) in various solvents at room temperature. (e) CD spectra of compound 8 (100 μM) in CH3OH at various temperatures.

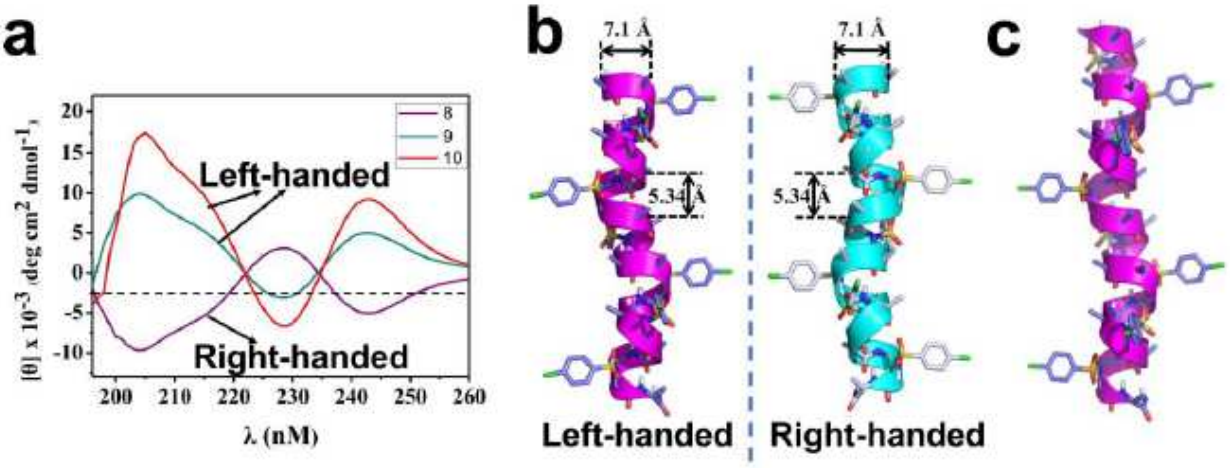

Figure 5

Left-handed foldamer (a) CD spectra of 1:1 D-α/D-sulfono-γ-AA hybrids 9 and 10 (100 μM) measured at room temperature in CH3OH, foldamer 8 was included as a mirror comparison. (b) Single-crystal structures of left-handed helix formed by D-15-mer 9. Single-crystal structures of right-handed helix formed by L-15-mer 8 was employed as a mirror comparison. (c) Single-crystal structures of left-handed helix formed by D-17-mer 10. The nonpolar hydrogens were omitted for clarity. Solvent molecules were also excluded from the crystal lattice.

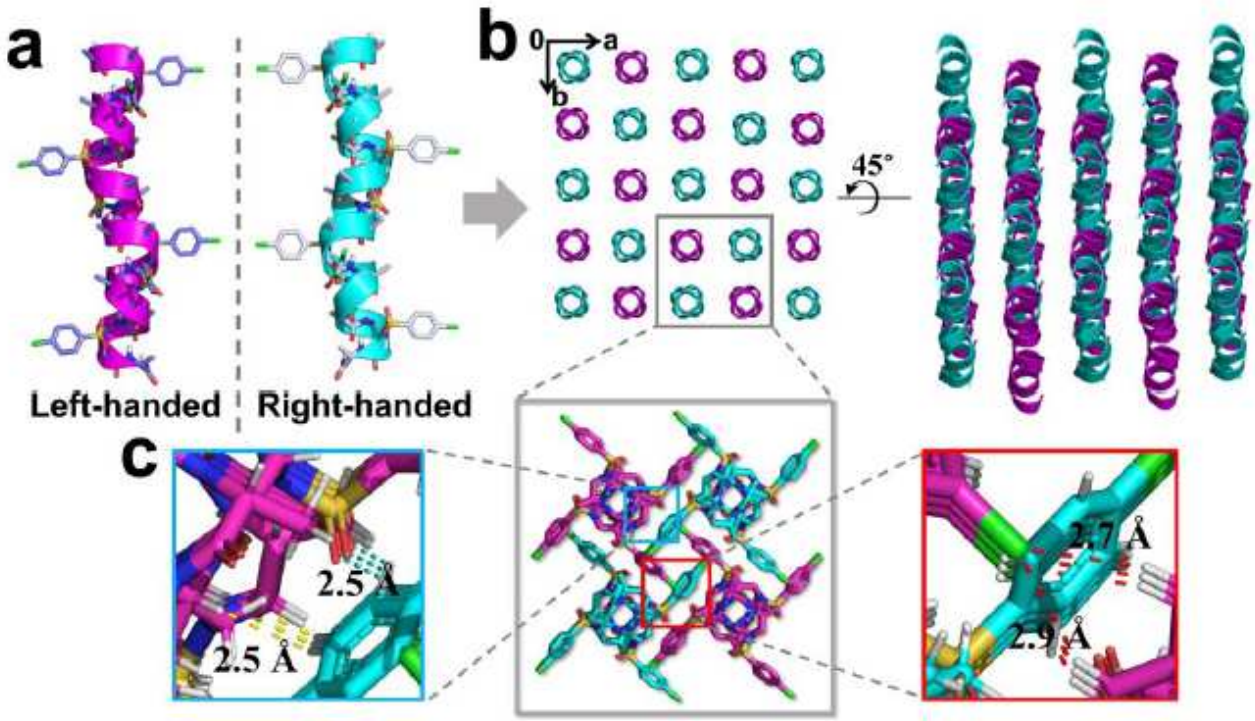

Figure 6

Crystal structure of the heterochiral coiled-coil-like 11. (a) Single-crystal structures of left-handed helix D-15-mer 9 and right-handed helix L-15-mer 8. (b) The crystal structures and crystal packing of heterochiral coiled-coil formed by racemic 15-mer 11. (c) Representative intermolecular interactions in the racemic crystals of 11. The intermolecular C=O···H□Ph and C□H···H□Ph interactions are indicated as cyan and yellow dashed line respectively. The interhelical C□H···Cl□Ph interactions are shown as red dashed line. Solvent molecules were excluded from the crystal lattice.

Supplementary Files

This is a list of supplementary files associated with this preprint. Click to download.

- Oligomer4.cif
- Oligomer6.cif
- Oligomer7.cif
- Oligomer9.cif
- Oligomer10.cif
- Racemate11.cif
- CheckcifOligomer4.pdf
- CheckcifOligomer6.pdf
- CheckcifOligomer7.pdf
- CheckcifOligomer9.pdf
- CheckcifOligomer10.pdf
- CheckcifRacemate11.pdf